Electronic Interactions of i, i+1 Dithioamides: Increased Fluorescence Quenching and Evidence for n-to-π* Interactions

Supplementary Information

Yun Huang,[a,b] John J. Ferrie,[a] Xing Chen,[a] Yitao Zhang,[a] D. Miklos Szantai-Kis,[a] David M. Chenoweth,[a] and E. James Petersson[a,*]

[a]Department of Chemistry, University of Pennsylvania, 213 South 34th Street, Philadelphia, PA 19104, USA.

[b]Current address: Department of Physiology and Biophysics, Weill Cornell Medical College, Cornell University, 1300 York Avenue, New York, NY 10065, USA

*ejpetersson@sas.upenn.edu

Table of Contents

General Information.

Fluorenyl methoxycarbonyl (Fmoc) protected amino acids, including alanine, leucine, (N^{ε}-*t*-butoxycarbonyl) lysine, glycine, phenylalanine, proline (*S*-*t*-butylthio) cysteine, and *p*-cyanophenylalanine, 2-chlorotrityl chloride resin were purchased from Novabiochem (San Diego, CA). Fmoc-β-(7-methoxycoumarin-4-yl)-alanine-OH was purchased from Bachem (Torrance, CA, USA). Fmoc-acridon-2-ylalanine was synthesized as previously described.[1] Piperidine and 2-(1-*H*-benzotriazol-1-yl)-1,1,3,3-tetramethyluronium hexafluorophosphate (HBTU) were purchased from American Bioanalytical (Natick, MA, USA). *N*,*N*-diisopropylethylamine (DIPEA), trifluoroacetic acid (TFA), 1,2-diamino-4-nitrobenzene and phosphorus pentasulfide (P_4S_{10}) were purchased from Sigma-Aldrich (St. Louis, MO, USA). 1,8-diazabicyclo[5.4.0]undec-7-ene (DBU) was purchased from Fisher Scientific. Trypsin (type II from porcine pancreas; 1,000 – 2,000 units/mg dry solid) was purchased from Sigma-Aldrich. Peptides were purified with a Varian ProStar High-Performance Liquid Chromatography (HPLC) instrument outfitted with a diode array detector (currently Agilent Technologies, Santa Clara, CA, USA) using aqueous (A: 0.1% TFA in H_2O) and organic (B: 0.1% TFA in acetonitrile) phases. Milli-Q filtered (18 MΩ) water was used for all solutions (Millipore; Billerica, MA, USA). Matrix-assisted laser desorption ionization mass spectrometry (MALDI MS) data were collected with a Bruker Ultraflex III mass spectrometer (Billerica, MA, USA). UV/Vis absorbance spectra were obtained with a Hewlett-Packard 8452A diode array spectrophotometer (currently Agilent Technologies). Fluorescence spectra were collected with a Tecan M1000 plate reader (San Jose, CA, USA) or a Photon Technologies International (PTI) QuantaMaster™ fluorometer (currently Horiba; Edison, NJ, USA). Proton (^{1}H) and carbon (^{13}C) NMR spectra were collected with a Bruker DRX 500 MHz spectrometer. High resolution mass spectrometry (HRMS) data were collected with a Waters LCT Premier XE operating in electrospray ionization (ESI) mode (Milford, MA, USA).

Synthesis of Thioamide Precursors.

The Fmoc-protected nitrobenzotriazole-activated amino thioacids were synthesized using a general procedure similar to those previously described.[2, 3]

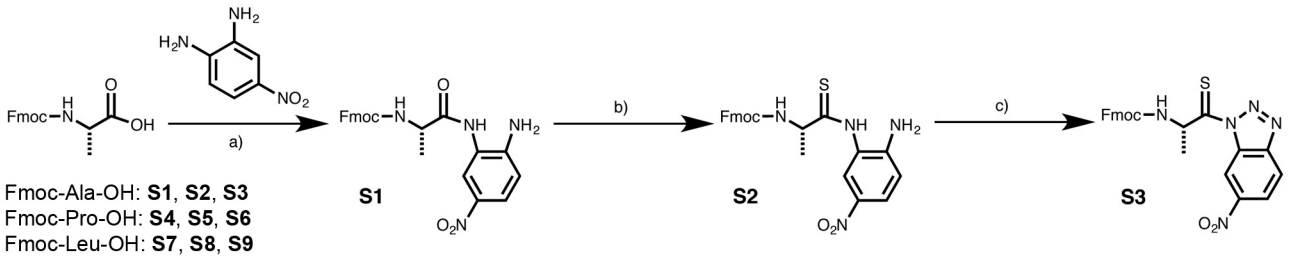

Scheme S1. Synthesis of Fmoc-Aminothioacylnitrobenzotriazolides. Synthesis of alanine derivative **S3** is shown as an example. Synthesis of proline and leucine derivatives **S6** and **S9** follow an identical procedure. a) isobutylchloroformate, -20 °C (1 h) to room temperature (3 h); b) P_4S_{10}, Na_2CO_3, 0 °C (0.5 h) to room temperature (2.5 h); c) AcOH, $NaNO_2$, 0 °C.

Coupling of Fmoc L-amino acids with 1,2-diamino-4-nitrobenzene. *N*-Methylmorpholine (2.2 ml, 20 mmol) was added to a solution of Fmoc-L-amino acid (10 mmol) in THF (100 ml) at -20 °C, followed by dropwise addition of isobutyl chloroformate (1.3 ml, 10 mmol). The mixture was stirred for 10 min, then 4-nitro-1,2-phenylenediamine (1.53 g, 10 mmol) was added, and the resulting slurry was stirred at -20 °C for 1 h and then at room temperature for 3 h. The precipitate was filtered off and the filtrate was evaporated to dryness. The residue was washed with EtOAc (250 ml) and the insoluble yellow solid was collected as pure product.

(9*H*-fluoren-9-yl)methyl (*S*)-(1-((2-amino-5-nitrophenyl)amino)-1-oxopropan-2-yl)carbamate (S1). Isolated yield 86%; R_f = 0.1 in 3:2 Hexanes/EtOAc; ^{1}H NMR (500 MHz, DMSO-d_6, major rotamer only) δ 9.43 (s, 1H), 8.21 (s, 1H), 7.88 – 7.68 (m, 6H), 7.41 (t, *J* = 7.5 Hz, 2H), 7.34 (t, *J* = 7.5 Hz, 2H), 6.80 (d, *J* = 9.0 Hz, 1H), 6.48 (s, 2H), 4.32 (d, *J* = 6.5 Hz, 2H), 4.25 (d, *J* = 6.0 Hz, 2H), 1.36 (d, *J* = 7.0 Hz, 3H); ^{13}C NMR (125 MHz, DMSO-d_6) δ 172.21, 156.08, 149.46, 143.91, 143.78, 140.76, 135.47, 127.67, 127.10, 125.33, 125.30, 123.19, 121.89, 121.23, 120.14, 113.61, 65.74, 50.67, 46.69, 17.72; HRMS (ESI) for $C_{24}H_{22}N_4O_5$ $[M+H]^+$ calcd.: 447.1663, found: 447.1671.

(9*H*-fluoren-9-yl)methyl (*S*)-2-((2-amino-5-nitrophenyl)carbamoyl)pyrrolidine-1-carboxylate (S4). Isolated yield 84%; R_f = 0.1 in 3:2 Hexanes/EtOAc; R_f = 0.70 in EtOAc; ^{1}H NMR (500 MHz, $CDCl_3$) δ 8.30 (s, 1H), 8.16 (s, 1H), 7.85 – 7.45 (m, 5H), 7.40 – 7.20 (m, 4H), 6.51 (d, *J* = 9.0 Hz, 1H), 4.85 (s,

2H), 6.48 (s, 2H), 4.45 – 4.15 (m, 4H), 3.60 – 3.40 (m, 2H) 2.32-1.80 (m, 4H); ^{13}C NMR (125 MHz, $CDCl_3$) δ 170.75, 156.19, 147.66, 143.52, 143.31, 141.15, 141.12, 137.75, 127.75, 127.11, 126.98, 124.90, 124.81, 123.57, 122.37, 120.84, 119.95, 119.93, 114.23, 67.81, 60.81, 47.13, 46.99, 28.89, 24.60, 18.83; HRMS (ESI) m/z for $C_{26}H_{24}N_4O_5$ $[M+H]^+$ calcd.: 473.1819, found: 473.1832.

(9*H*-fluoren-9-yl)methyl (*S*)-(1-((2-amino-5-nitrophenyl)amino)-4-methyl-1-oxopentan-2-yl) carbamate (S7). The compound was isolated in quantitative yield and 94.9% purity, as determined by HPLC; ^{1}H NMR (500 MHz, DMSO-d_6) δ 9.57 (s, 1H), 8.24 (d, J = 2.2 Hz, 1H), 7.91 – 7.84 (m, 3H), 7.79 (d, J = 7.6 Hz, 1H), 7.75 (d, J = 7.5 Hz, 2H), 7.41 (t, J = 7.5 Hz, 2H), 7.32 (t, J = 7.5 Hz, 2H), 6.79 (d, J = 9.1 Hz, 1H), 6.56 (s, 2H), 4.37 – 4.21 (m, 3H), 1.76 – 1.65 (m, 1H), 1.67 – 1.56 (m, 1H), 0.95 (d, J = 6.4 Hz, 3H), 0.92 (d, J = 6.5 Hz, 3H); ^{13}C NMR (125 MHz, DMSO) δ 172.13, 156.22, 149.19, 143.85, 143.73, 140.70, 135.45, 127.61, 127.03, 125.31, 122.97, 121.54, 121.29, 120.07, 113.67, 65.68, 53.73, 46.69, 40.25, 24.33, 23.03, 21.56; HRMS (ESI) m/z for $C_{27}H_{29}N_4O_5$ $[M+H]^+$ calcd.: 489.2132, found: 489.2148.

Preparation of Fmoc L-amino thioacid nitroanilides. P_4S_{10} (0.88 g, 2 mmol) was mixed with Na_2CO_3 (0.216 g, 2 mmol) in THF (100 ml). The mixture was stirred under an argon atmosphere for 1 h at room temperature and then cooled to 0 °C. To this clear solution was added *N*-Fmoc L-amino acid-2-amino-5-nitroanilide (4 mmol), and the reaction mixture was stirred at 0 °C for 30 min and then at room temperature for 2.5 h. The mixture was filtered and the filtrate was evaporated to dryness. The residue was dissolved in EtOAc and washed with 5% $NaHCO_3$ (2 · 30 ml) and the aqueous layers were back-extracted with EtOAc (75 ml). The combined organic layers were washed with brine, dried over $MgSO_4$, and evaporated to yellow solid. Further purification was conducted by silica gel column chromatography with elution in hexane/EtOAc.

(9*H*-fluoren-9-yl)methyl (*S*)-(1-((2-amino-5-nitrophenyl)amino)-1-thioxopropan-2-yl)carbamate (S2). Isolated yield 80%; R_f = 0.1 in 3:2 Hexanes/EtOAc; ^{1}H NMR (500 MHz, DMSO-d_6) δ 11.28 (s, 1H), 7.98 (m, 2H), 7.93 (d, J = 2.0 Hz, 1H), 7.90 (d, J = 7.5 Hz, 2H), 7.81-7.70 (m, 2H), 7.40, (t, J = 7.5 Hz, 2H), 7.33 (t, J = 7.5 Hz, 2H), 6.80 (d, J = 9.0 Hz, 1H), 6.42 (s, 2H), 4.56 (t, J = 6.0 Hz, 1H) 4.40 – 4.20 (m, 3H) 1.47 (d, J = 7.0 Hz, 3H); ^{13}C NMR (125 MHz, DMSO-d_6) δ 208.36, 156.22, 150.72, 143.90, 143.63, 140.73, 140.71, 135.31, 127.68, 127.11, 127.08, 125.41, 125.28, 124.99, 124.79, 122.42,

120.12, 113.89, 65.89, 56.98, 46.63, 20.30; HRMS (ESI) for $C_{24}H_{22}N_4O_4S$ $[M+H]^+$ calcd.: 463.1435, found 463.1435.

(9*H*-fluoren-9-yl)methyl (*S*)-2-((2-amino-5-nitrophenyl)carbamothioyl)pyrrolidine-1-carboxylate (S5). Isolated yield 71%; R_f = 0.3 in 3:2 Hexanes/EtOAc; ^{1}H NMR (500 MHz, $CDCl_3$) δ 9.05 (s, 1H), 8.00 (s, 1H), 7.92 (d, *J* = 9.0 Hz, 1H) 7.75 (d, *J* = 7.5 Hz, 2H), 7.55 (d, *J* = 7.0 Hz, 2H), 7.40-7.20 (m, 4H), 6.58 (d, *J* = 9.0 Hz, 1H), 5.01 (s, 2H), 4.75 – 4.15 (m, *4*H), 3.60 – 3.40 (m, 2H) 2.42-1.80 (m, 4H); ^{13}C NMR (125 MHz, $CDCl_3$) δ 205.45, 156.15, 149.06, 143.45, 143.39, 141.22, 141.17, 137.51, 127.79, 127.10, 127.01, 125.56, 125.17, 124.87, 124.81, 121.63, 119.99, 114.45, 68.45, 67.77, 47.69, 47.06, 33.12, 24.41; HRMS (ESI) m/z for $C_{26}H_{24}N_4O_4S$ $[M+H]^+$ calcd.: 489.1591, found 489.1608.

(9*H*-fluoren-9-yl)methyl (*S*)-(1-((2-amino-5-nitrophenyl)amino)-4-methyl-1-thioxopentan-2-yl) carbamate (S8). Isolated yield 68.4%; Rf = 0.5 in EtOAc/Hexanes (1:1); ^{1}H NMR (500 MHz, Chloroform-*d*) δ 9.65 (s, 1H), 7.99 (s, 1H), 7.92 (dd, *J* = 9.0, 2.6 Hz, 1H), 7.72 (t, *J* = 6.9 Hz, 2H), 7.48 (d, *J* = 7.5 Hz, 1H), 7.43 (d, *J* = 7.6 Hz, 1H), 7.40 – 7.30 (m, 2H), 7.29 – 7.18 (m, 2H), 6.56 (d, *J* = 9.0 Hz, 1H), 5.69 (d, *J* = 7.5 Hz, 1H), 4.66 (d, *J* = 8.5 Hz, 1H), 4.61 (s, 2H), 4.26 (d, *J* = 7.3 Hz, 2H), 4.11 (t, *J* = 7.2 Hz, 1H), 1.87 – 1.80 (m, 1H), 1.79 – 1.72 (m, 2H), 0.99 (t, *J* = 6.0 Hz, 6H); ^{13}C NMR (125 MHz, $CDCl_3$) δ 206.93, 157.20, 148.61, 143.37, 143.28, 141.29, 141.23, 138.18, 128.00, 127.93, 127.36, 127.22, 125.57, 124.92, 124.85, 122.27, 120.20, 120.14, 115.17, 67.57, 60.45, 46.92, 44.28, 25.05, 22.80, 22.27; HRMS (ESI) m/z for $C_{27}H_{29}N_4O_4S^+$ $[M+H]^+$ calcd.: 505.1904, found: 505.1916.

Preparation of Fmoc L-amino thioacid nitrobenzotriazolides. To a solution of Fmoc L-amino acid thioanilide (0.5 mmol), dissolved by gentle warming at 40 °C and then cooled to 0 °C in glacial acetic acid (30 ml), $NaNO_2$ was added (0.052 g, 0.75 mmol) in portions over 5 min under constant stirring. After 30 min, ice-cold water (100 ml) was added and the precipitated product was filtered and washed thoroughly with water. The orange solid was extracted with DCM and dried over $MgSO_4$ and evaporated to dryness. The product was used in peptide coupling without further purification. Silica gel column chromatography was used to purify samples for NMR analysis.

(9*H*-fluoren-9-yl)methyl (*S*)-(1-(6-nitro-1*H*-benzo[*d*][1,2,3]triazol-1-yl)-1-thioxopropan-2-yl) carbamate (S3). Isolated yield 73%; R_f = 0.7 in 3:2 Hexanes/EtOAc; ^{1}H NMR (500 MHz, $CDCl_3$, major rotamer only) δ 9.54 (s, 1H), 8.43 (d, *J* = 8.5 Hz, 1H), 8.30 (d, *J* = 9.0 Hz, 1H), 7.81-6.90 (m, 8H), 6.26 (m, 1H), 5,79 (m, 1H), 4.60 – 4.00 (m, 3H) 1.69 (d, *J* = 6.5 Hz, 3H); ^{13}C NMR (125 MHz, $CDCl_3$,

major rotamer only) δ 210.06, 155.43, 149.50, 148.89, 143.63, 143.56, 141.24, 131.85, 127.70, 127.02, 125.03, 124.91, 122.16, 121.44, 119.94, 112.74, 66.96, 57.35, 47.10, 22.49; HRMS (ESI) for $C_{24}H_{19}N_5O_4S$ $[M+H]^+$ calcd.: 474.1231, found: 474.1242.

(9*H*-fluoren-9-yl)methyl (*S*)-2-(6-nitro-1*H*-benzo[*d*][1,2,3]triazole-1-carbonothioyl)pyrrolidine-1-carboxylate (S6). Isolated yield 70%; R_f = 0.5 in 3:2 Hexanes/EtOAc; ^{1}H NMR (500 MHz, CD_2Cl_2, major rotamer only) δ 9.50 (s, 1H), 8.54-8.30 (m, 2H), 7.86-6.79 (m, 8H), 5.64 (m, 1H), 4.76 – 4.32 (m, 2H), 4.32 – 3.50 (m, 3H) 2.72-1.80 (m, 4H); ^{13}C NMR (125 MHz, CD_2Cl_2, major rotamer only) δ 207.12, 154.14, 150.01, 149.39, 144.40, 144.36, 141.47, 132.55, 128.24, 127.64, 127.31, 127.33, 125.71, 124.59, 122.61, 121.85, 120.49, 119.65, 67.83, 65.67, 47.75, 34.60, 23.10; HRMS (ESI) m/z for $C_{26}H_{21}N_5O_4S$ $[M+H]^+$ calcd.: 500.1387, found: 500.1399.

(9*H*-fluoren-9-yl)methyl (*S*)-(4-methyl-1-(6-nitro-1*H*-benzo[*d*][1,2,3]triazol-1-yl)-1-thioxopentan-2-yl)carbamate (S9). Isolated yield: 89.5%; R_f = 0.2 in CH_2Cl_2; ^{1}H NMR (500 MHz, $CDCl_3$, major rotamer only) δ 9.66 (s, 1H), 8.44 (dd, *J* = 8.9, 2.1 Hz, 1H), 8.31 (d, *J* = 8.9 Hz, 1H), 7.82 – 7.71 (m, 2H), 7.61 (d, *J* = 7.5 Hz, 2H), 7.40 (t, *J* = 5.6 Hz, 2H), 7.32 (q, *J* = 7.2 Hz, 2H), 6.37 – 6.24 (m, 1H), 5.63 (d, *J* = 9.6 Hz, 1H), 4.54 (dd, *J* = 10.8, 6.7 Hz, 1H), 4.40 (dd, *J* = 10.9, 6.9 Hz, 1H), 4.22 (t, *J* = 6.8 Hz, 1H), 1.96 – 1.86 (m, 1H), 1.86 – 1.65 (m, 2H), 1.26 (s, 2H), 1.13 (d, *J* = 6.4 Hz, 3H), 0.97 (d, *J* = 6.6 Hz, 3H); ^{13}C NMR (125 MHz, $CDCl_3$, major rotamer only) δ 210.70, 156.05, 149.70, 149.14, 143.74, 141.48, 132.04, 127.87, 127.20, 125.19, 125.09, 122.31, 121.61, 120.13, 112.94, 67.06, 47.40, 46.05, 25.87, 23.45, 21.45; HRMS (ESI) m/z for $C_{27}H_{25}N_5O_4S$ $[M+Na]^+$ calcd.: 538.1519, found: 538.1535.

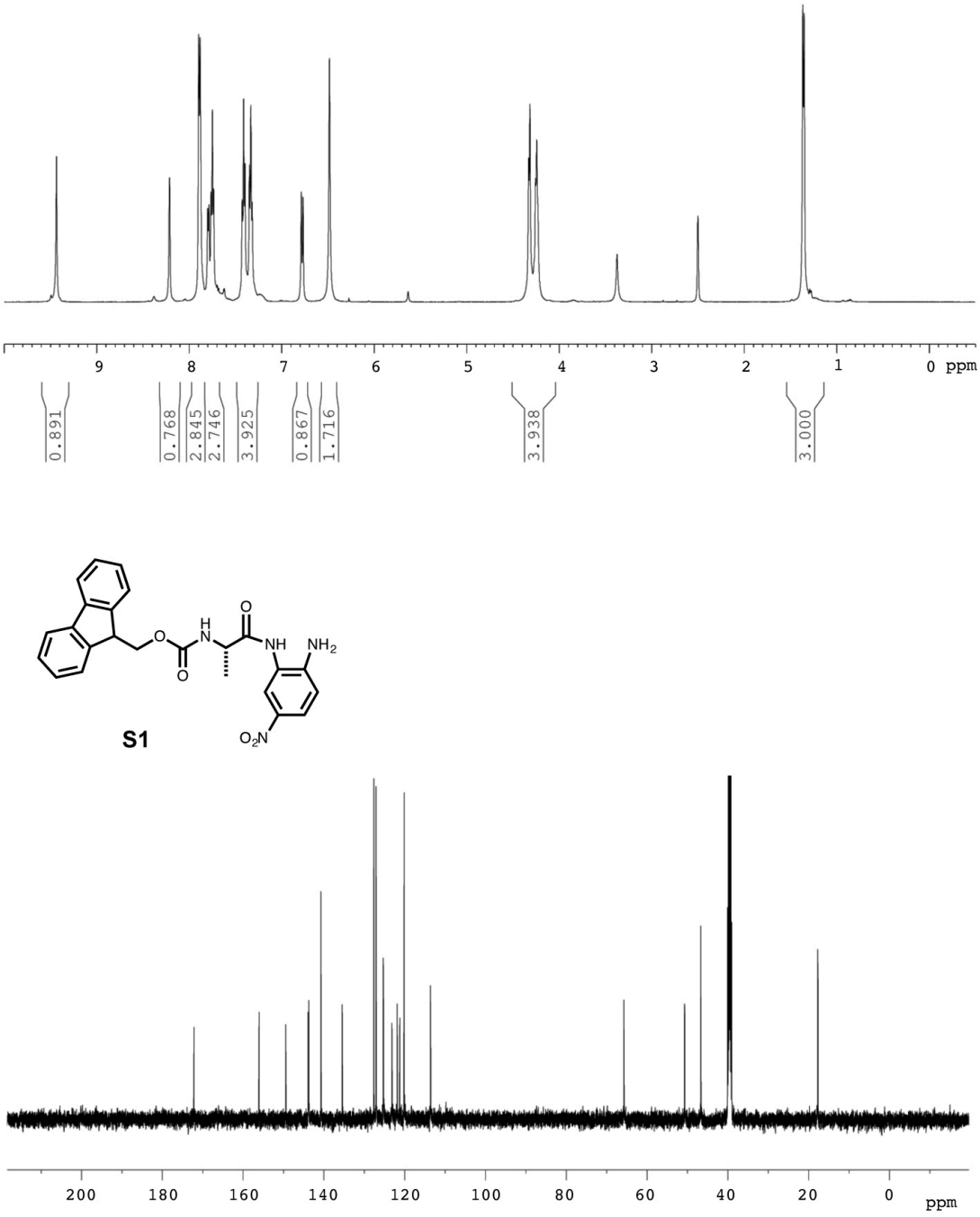

Fig. S1. ^{1}H and ^{13}C NMR Spectra of (9*H*-fluoren-9-yl)methyl (*S*)-(1-((2-amino-5-nitrophenyl)amino)-1-oxopropan-2-yl)carbamate (**S1**) in DMSO-d_6.

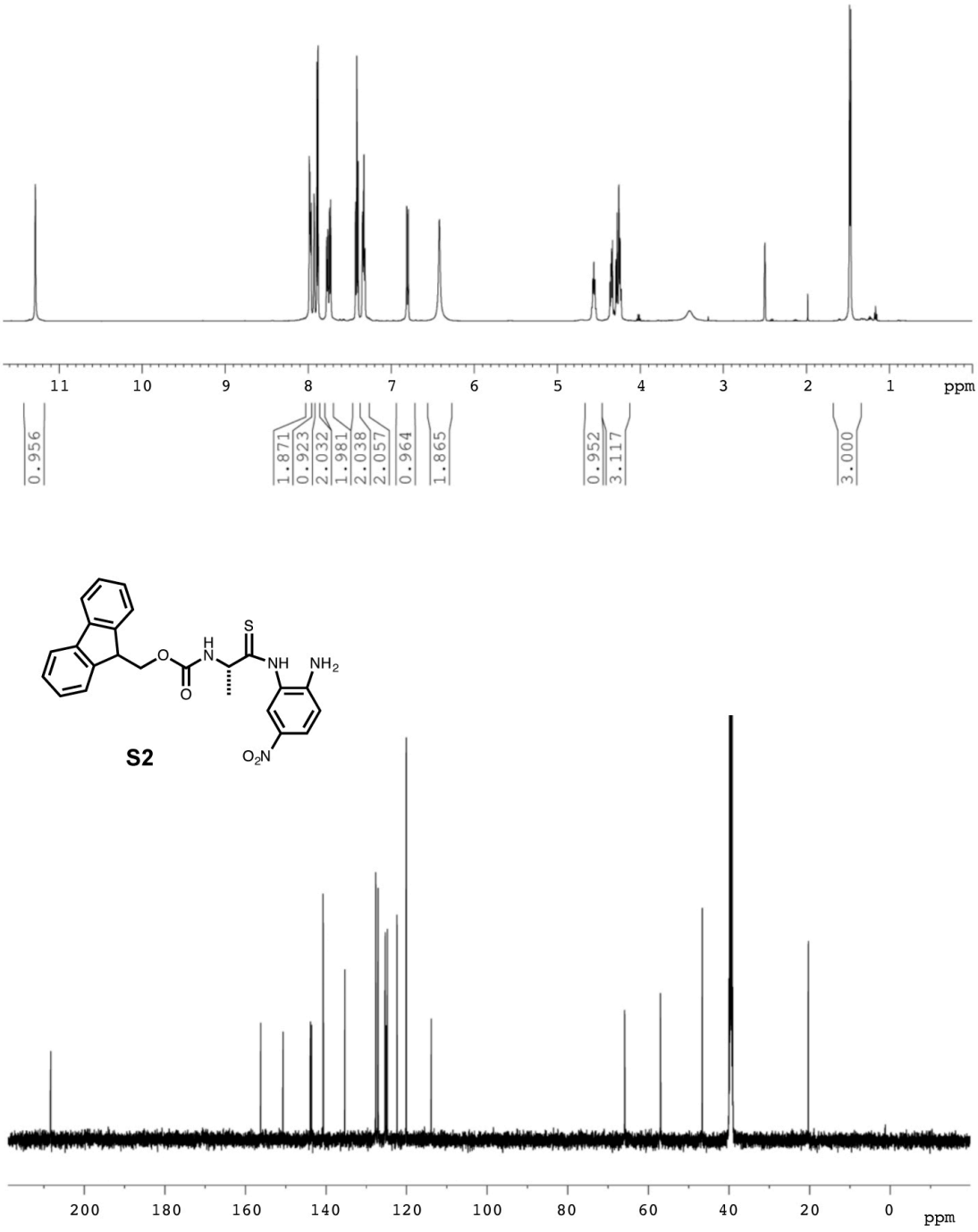

Fig. S2. ^{1}H and ^{13}C NMR Spectra of (9*H*-fluoren-9-yl)methyl (*S*)-(1-((2-amino-5-nitrophenyl)amino)-1-thioxopropan-2-yl)carbamate (**S2**) in DMSO-d_6.

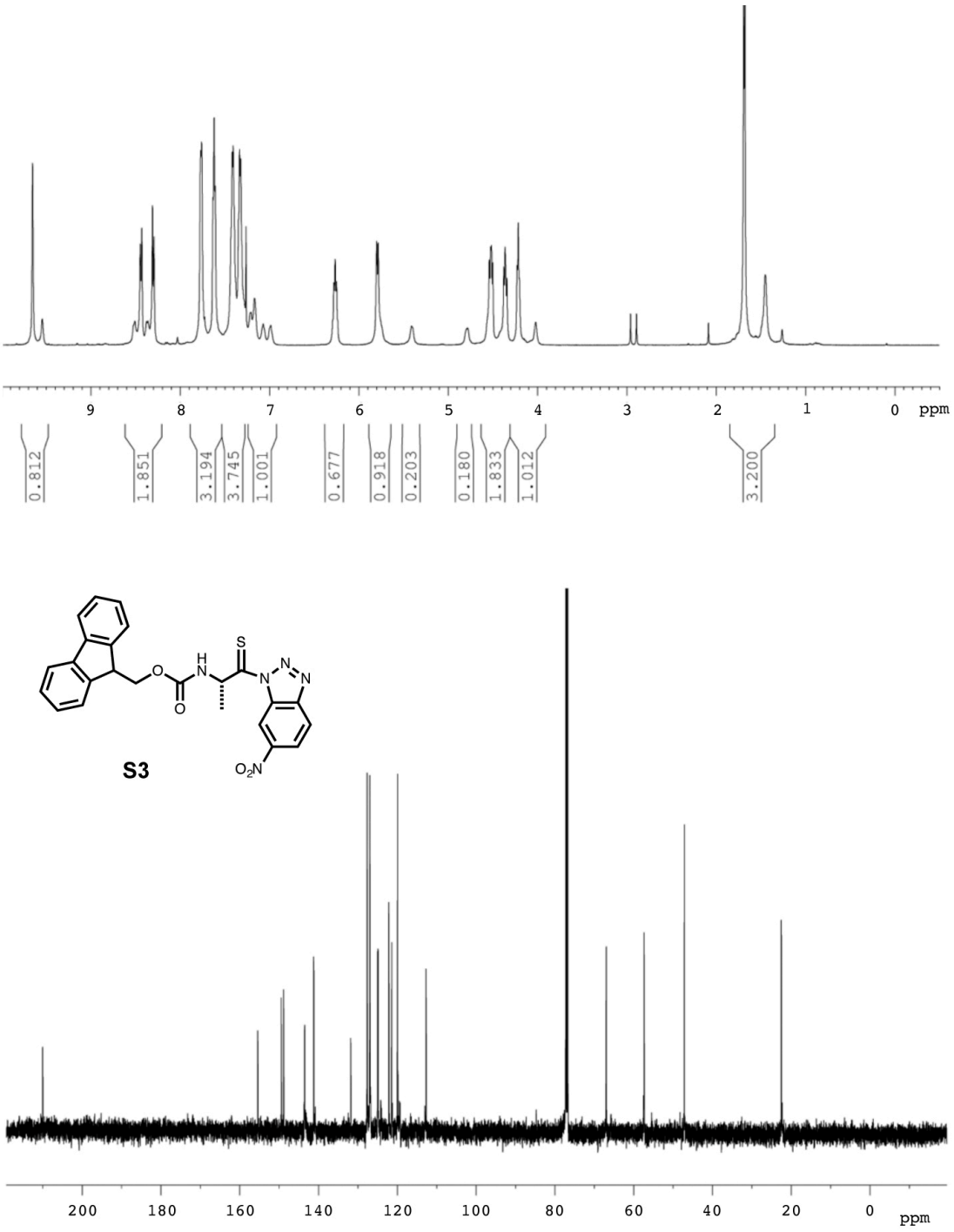

Fig. S3. ^{1}H and ^{13}C NMR Spectra (9*H*-fluoren-9-yl)methyl (*S*)-(1-(6-nitro-1*H*-benzo[*d*][1,2,3]triazol-1-yl)-1-thioxopropan-2-yl)carbamate (**S3**) in $CDCl_3$.

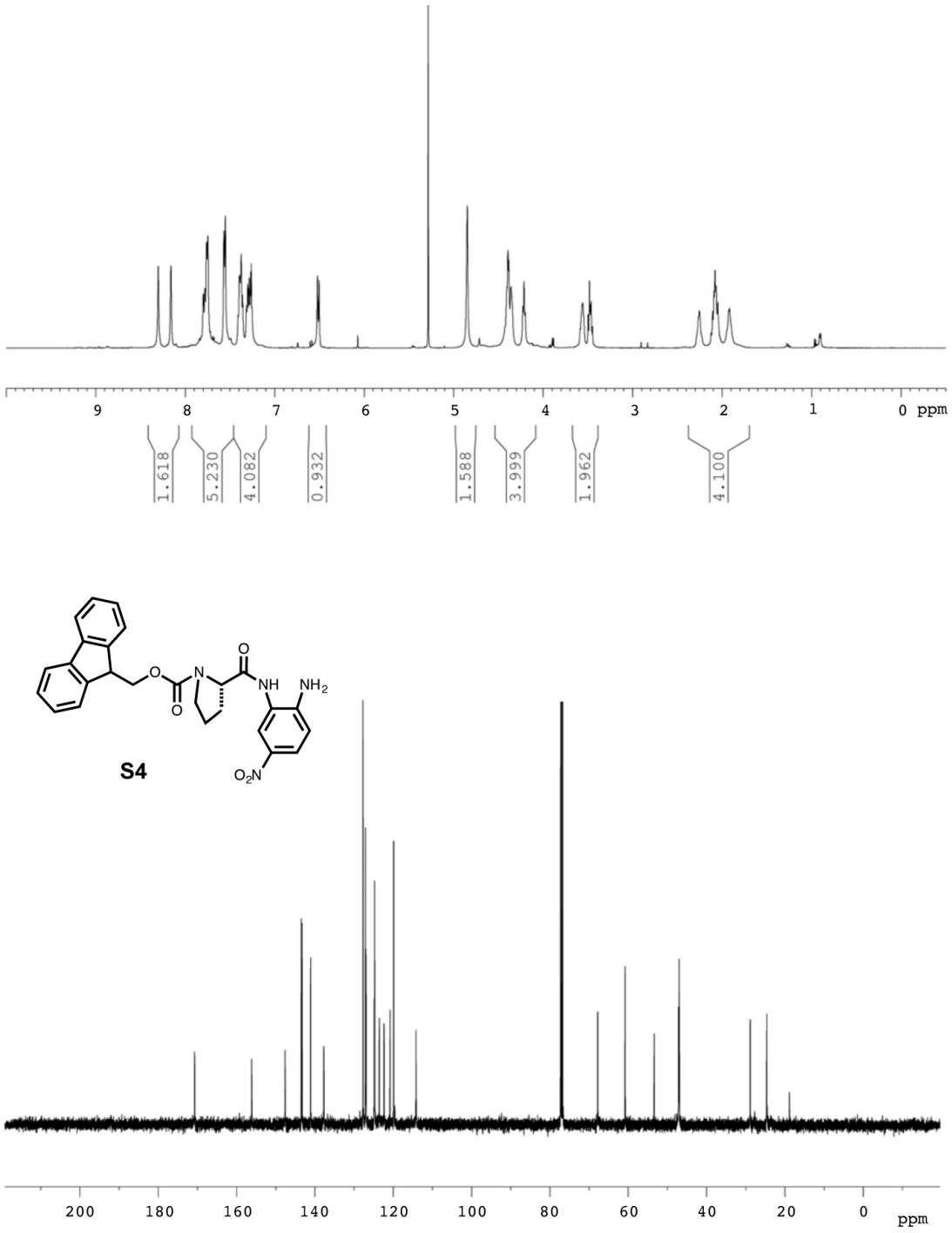

Fig. S4. ^{1}H and ^{13}C NMR Spectra of (9*H*-fluoren-9-yl)methyl (*S*)-2-((2-amino-5-nitrophenyl)carbamoyl)pyrrolidine-1-carboxylate (**S4**) in DMSO-d_6.

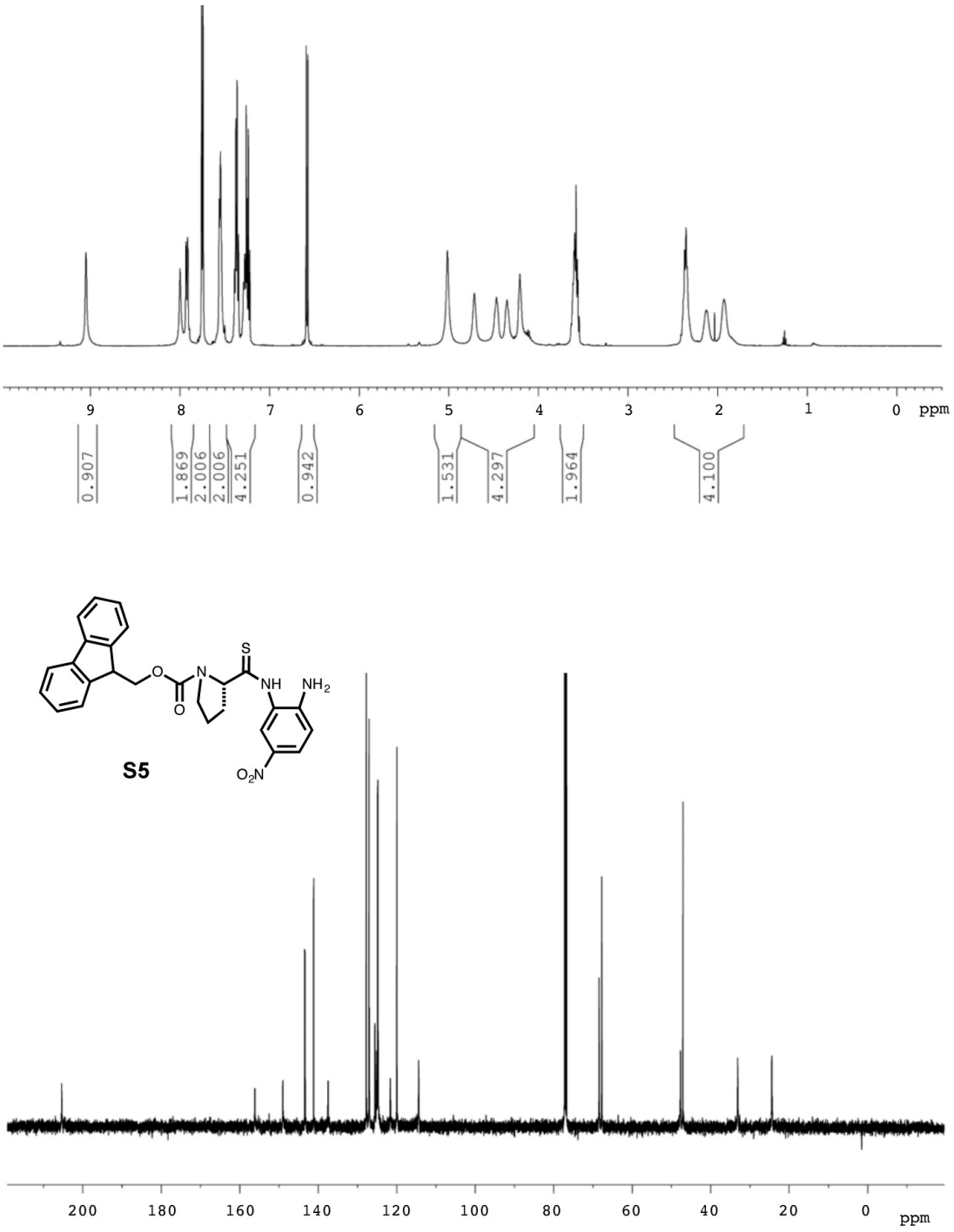

Fig. S5. ^{1}H and ^{13}C NMR Spectra of (9*H*-fluoren-9-yl)methyl (*S*)-2-((2-amino-5-nitrophenyl)carbamothioyl) pyrrolidine-1-carboxylate (**S5**) in DMSO-d_6.

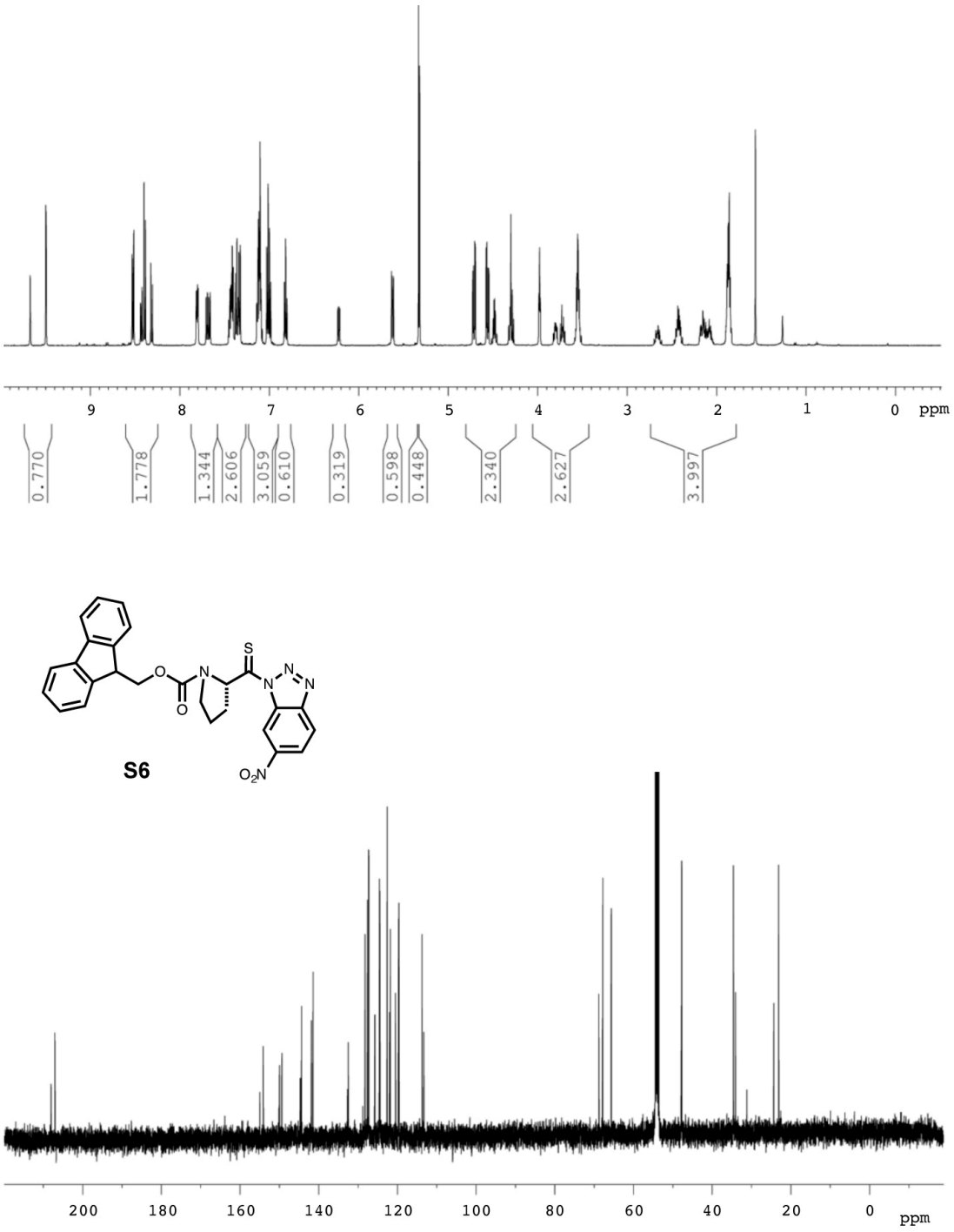

Fig. S6. ^{1}H and ^{13}C NMR Spectra of (9*H*-fluoren-9-yl)methyl (*S*)-2-(6-nitro-1*H*-benzo[*d*][1,2,3]triazole-1-carbonothioyl)pyrrolidine-1-carboxylate (**S6**) in CD_2Cl_2.

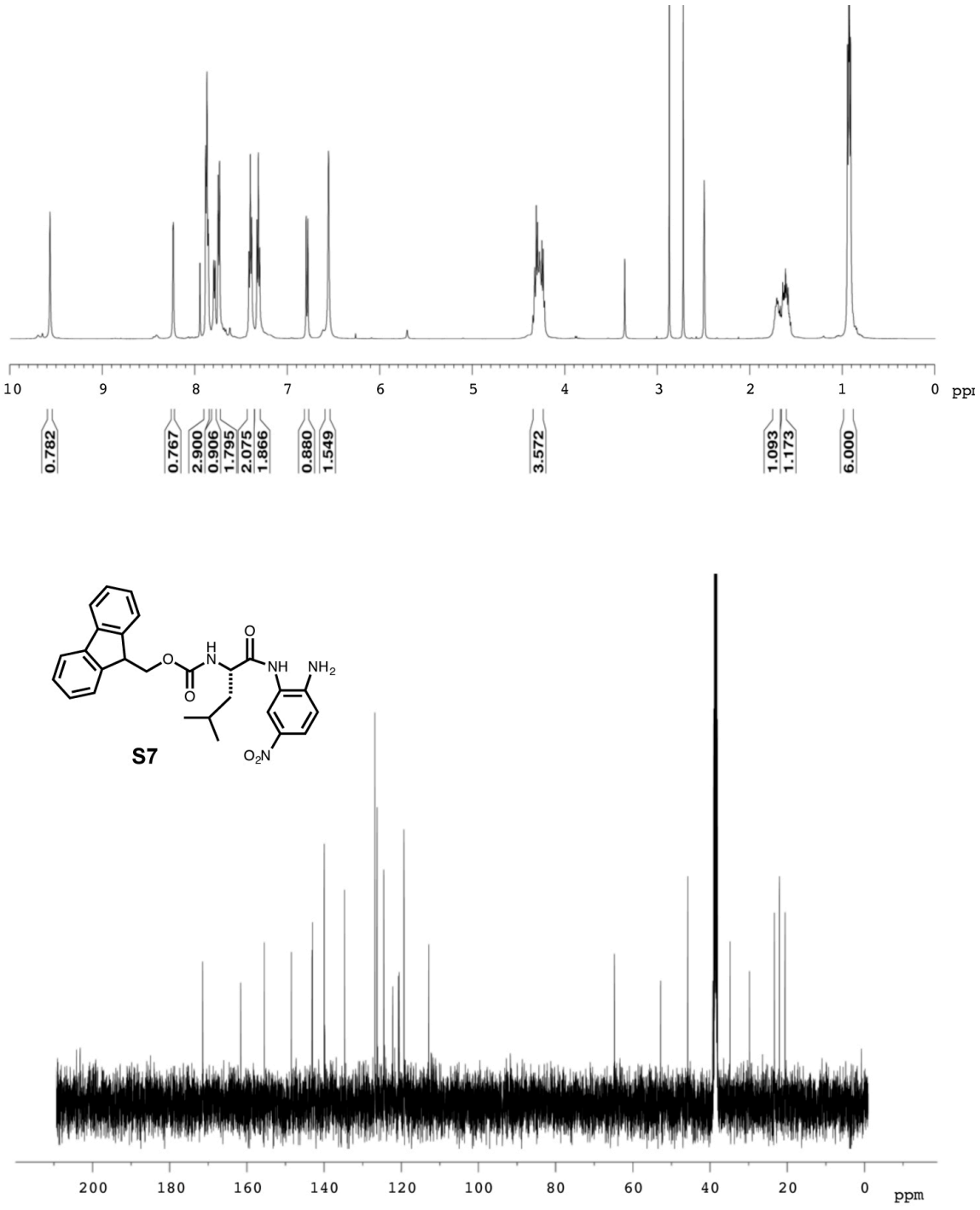

Fig. S7. ^{1}H and ^{13}C NMR Spectra of (9*H*-fluoren-9-yl)methyl (*S*)-(1-((2-amino-5-nitrophenyl)amino)-4-methyl-1-oxopentan-2-yl) carbamate (**S7**) in DMSO-d_6.

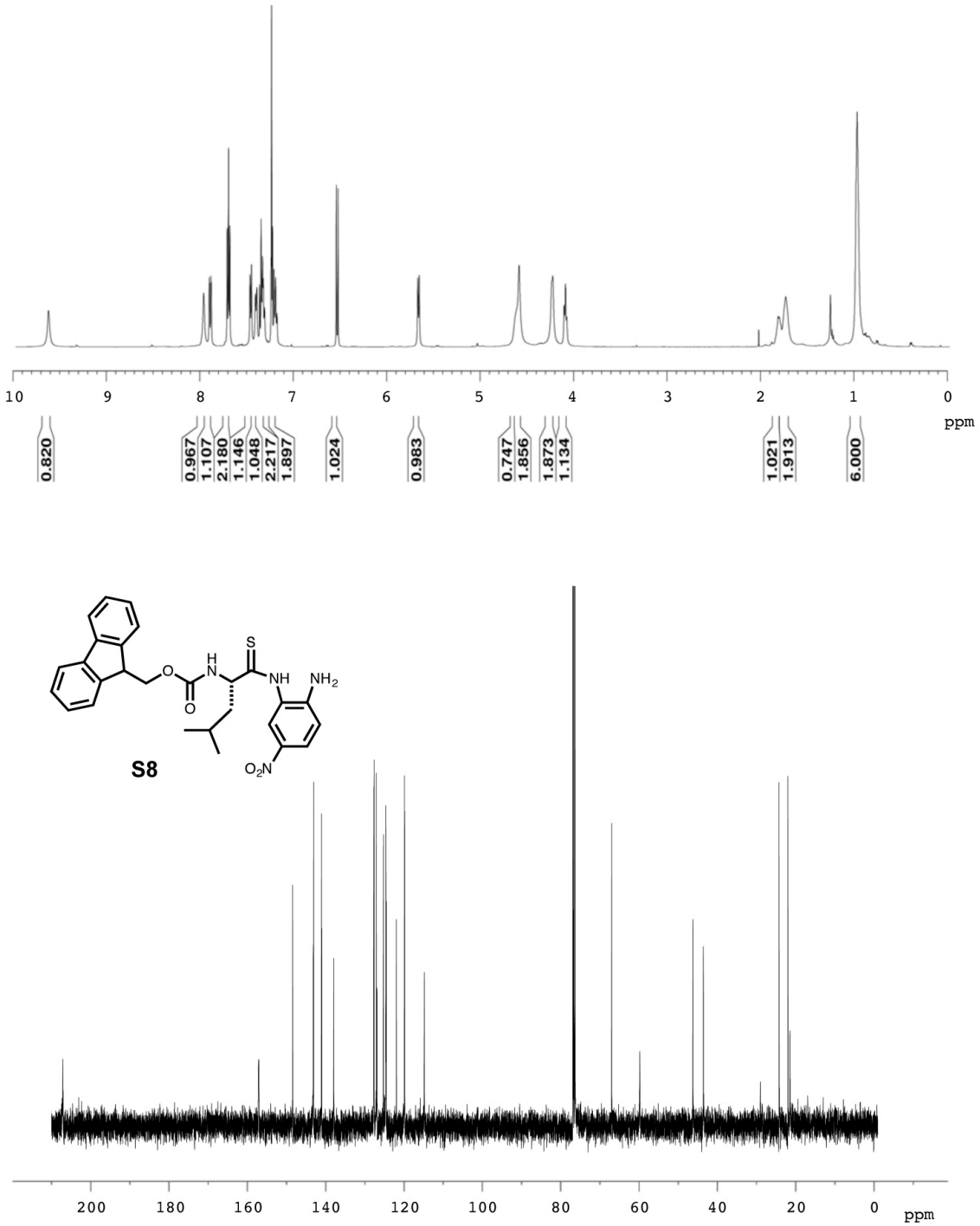

Fig. S8. ^{1}H and ^{13}C NMR Spectra of (9*H*-fluoren-9-yl)methyl (*S*)-(1-((2-amino-5-nitrophenyl)amino)-4-methyl-1-thioxopentan-2-yl)carbamate (**S8**) in DMSO-d_6.

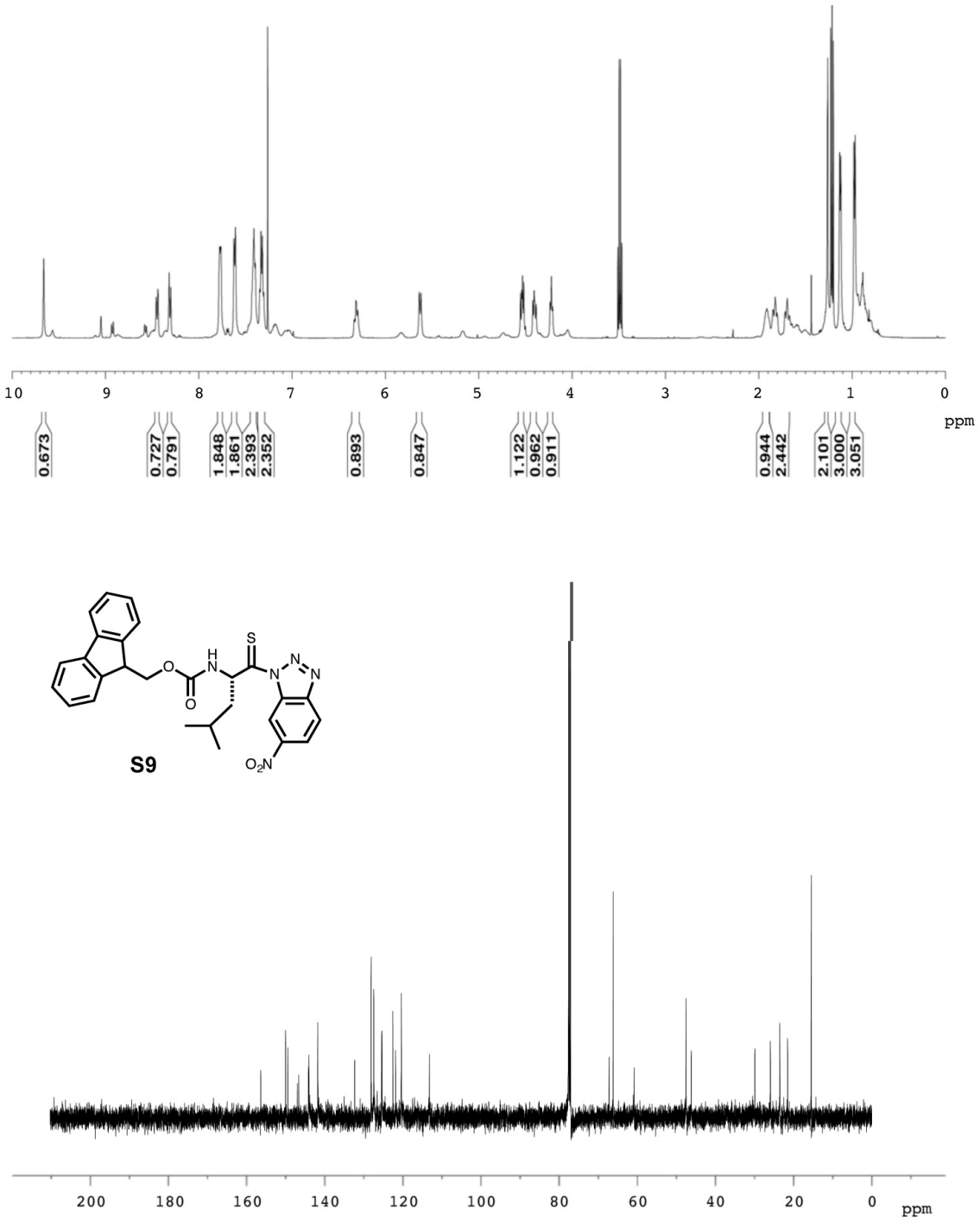

Fig. S9. ^{1}H and ^{13}C NMR Spectra of (9*H*-fluoren-9-yl)methyl (*S*)-(4-methyl-1-(6-nitro-1*H*-benzo[*d*][1,2,3]triazol-1-yl)-1-thioxopentan-2-yl)carbamate (**S9**) in CD_2Cl_2.

Peptide Synthesis.

The peptides were manually synthesized with fritted syringes (Torviq; Niles, MI, USA) with an Fmoc-based strategy. For a typical synthesis, 20 mg 2-chlorotrityl resin (100-200 mesh; 1.5 mmol substitution/g) was added to a 10 ml syringe. Dry dichloromethane (DCM, 2 ml) was added and incubated for 30 min under magnetic stirring to swell the resin. After swelling, DCM was removed and the first Fmoc-amino acid (1 equiv) in 2 mL DCM and DIPEA (4 equiv) was added to the syringe. The mixture was allowed to react for 40 min and then the resin was washed with DMF four times. MeOH capping was performed to block unreacted resin sites by washing three times with DCM/MeOH/DIPEA (17:2:1), three times with DCM, and three times with DMF. The Fmoc group was removed by treatment with 20% piperidine in DMF (2 mL) for 20 min with magnetic stirring. The deprotection solution was collected and the Fmoc content was determined by absorbance at 300 nm (ε_{300} = 7800).[4] Subsequent amino acid couplings were performed by adding Fmoc-amino acid (5 equiv) in 2 mL DMF with HBTU (5 equiv) and DIPEA (10 equiv) and stirring for 30 min. For the thioamide peptides, the thioamide-containing amino acids were introduced by adding 3 equiv Fmoc-thioacylbenzotriazolide (**S3**, **S6**, **S9**) in 2 mL dry DCM with 1 equiv DIPEA and incubating for 2 hours. The following Fmoc deprotections were conducted by treating the resin with freshly prepared 2% DBU/1% HOBt/dry DMF (v/w/v) for 30 s, repeated three times. Note: Use of the DBU deprotection cocktail avoided epimerization observed when using the standard 20% piperidine deprotection solution. An example of epimerization observed by HPLC is shown in Fig. S1. After chain elongation, the peptides were cleaved by treating with acetic acid/trifluoroethanol (TFE)/DCM (2/2/6, v/v/v) for 2 h. The resulting solution was expelled from the syringe and evaporated under reduced pressure.

The peptides were purified to homogeneity by reverse-phase HPLC on a Vydac 218TP C18 semi-prep or preparative column (Grace/Vydac; Deerfield, IL, USA) with MeCN/H_2O (0.1% TFA) eluent system and monitoring the absorbance at 215 nm. MALDI-MS was used to confirm peptide identities. (Table S1) Purified peptides were lyophilized and stored at -20 °C.

For the synthesis of fluorescein-labeled peptides, C(S-*t*Bu)PPPPA^{x}A^{x}G (X = O, or S) peptides were synthesized using Fmoc-(*S*-*t*-butylthio)-cysteine at the N-terminus, purified and re-dissolved in 20 mM sodium phosphate buffer containing 10% acetonitrile, to which was added 10 equiv tris(2-carboxyethyl)phosphine (TCEP) and, 10 min later, 5 equiv fluorescein-5-maleimide in DMSO. The reaction was conducted for 3 h at room temperature and then subjected to HPLC purification.

Table S1. Calculated and Observed Peptide Masses.

	Peptide	Calcd. $[M+H]^+$	m/z Found
1	μP_3PAAG	851.39	851.43
2	μP_3P^sAAG	867.36	889.39 ($[M+Na]^+$)
3	μP_3PA^sAG	867.36	889.39 ($[M+Na]^+$)
4	μP_3PAA^sG	867.36	867.41
5	$\mu P_3PA^sA^sG$	883.34	883.38
6	$\mu P_3P^sAA^sG$	883.34	883.36
7	$\mu P_3P^sA^sA^sG$	890.32	921.08 ($[M+Na]^+$)
8	F^*PPAAG	584.28	584.49
9	F^*PPA^sAG	600.25	600.49
10	$F^*PPA^sA^sG$	616.23	616.42
11	$F^*P_3PA^sA^sG$	810.34	810.35
12	$F^*P_3P^sA^sA^sG$	826.31	826.05
13	$\mu PPAAG$	657.28	679.37 ($[M+Na]^+$)
14	$\mu PPAA^sG$	673.26	673.38
15	μPPA^sAG	673.26	695.38 ($[M+Na]^+$)
16	μPPA^sA^sG	689.23	689.38
17	δP_3PAAG	870.41	870.40
18	δP_3PAA^sG	886.39	886.77
19	δP_3PA^sAG	886.39	886.85
20	$\delta P_3PA^sA^sG$	902.36	902.46
21	ψP_3PAAG	1136.40	1136.52
22	ψP_3PAA^sG	1152.37	1152.49
23	ψP_3PA^sAG	1152.37	1152.50
24	$\psi P_3PA^sA^sG$	1168.35	1168.44
25	$ALLKAA\mu$	831.45	831.26
26	$A^sLLKAA\mu$	847.43	847.28
27	$AL^sLKAA\mu$	847.43	847.30
28	$A^sL^sLKAA\mu$	863.41	863.22
29	$FPPPPA^sA^sG$	785.34	785.41
30	$FPPPP^sA^sA^sG$	801.33	801.45

F^* is *p*-cyanophenylalanine; μ is 7-methoxycoumarin-4-ylalanine; δ is acridon-2-ylalanine; ψ is fluorescein-5-maleimide attached on a cysteine side-chain; ^{s} represents a thioamide bond.

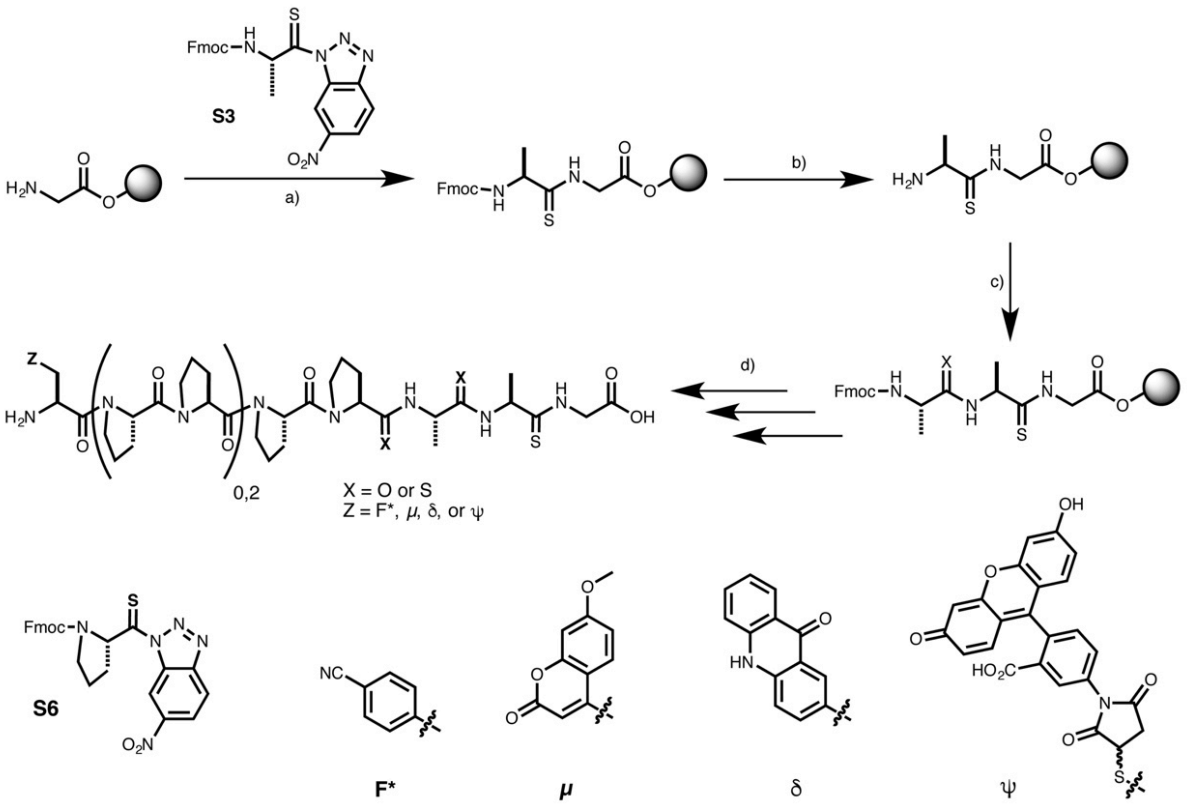

Scheme S2. Synthesis of Thioamide Peptides. a) DIPEA, dry DCM; b) 2% DBU/1% HOBt, DMF; c) For a thioalanine unit: **S3**, DIPEA, dry DCM; For an alanine unit: Fmoc-Ala-OH, DIPEA, HBTU, DMF; d) Repeat c) and d) with various Fmoc amino acids or thioamide precursors to complete peptide; cleave from resin with 2/2/6 AcOH/TFE/DCM.

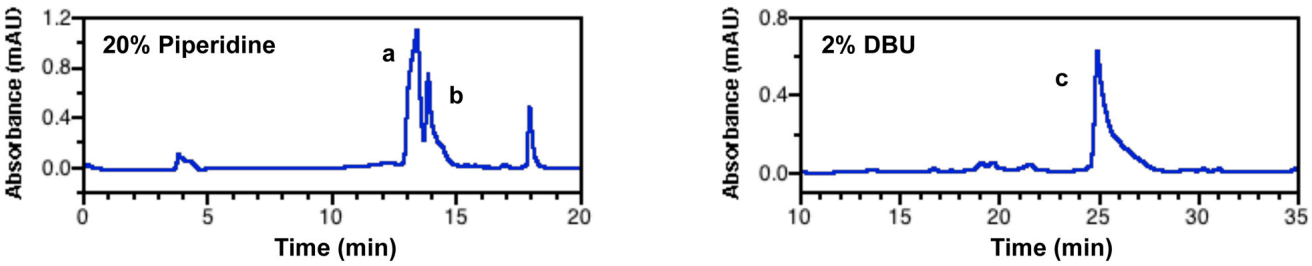

Fig. S10 Dithioamide Epimerization with 20% Piperidine Treatment. HPLC analysis of F*PPA^{s}A^{s}G synthesized by different Fmoc deprotection methods: 20% piperidine/DMF, 20 min (Left, Vydac 218TP C18 analytical column, eluting with 5% CH_3CN for 2 min and then increasing to 65% CH_3CN over 20 min, flow rate: 1ml/min) and 2% DBU/1% HOBt/DMF, 3 X 40 s (Right, Vydac 218TP C18 semi-prep column, eluting with 5% CH_3CN for 2 min and then increasing to 35% CH_3CN over 35 min, flow rate: 4 ml/min). The 20% piperidine treatment resulted in epimerization (peaks a and b contain peptides of the same parent m/z, 616.4 $[M+H]^+$, and fragmentation pattern).

UV/Vis and Fluorescence Spectroscopy of Polyproline Peptides.

UV/Vis Spectroscopy. All UV/Vis spectra were collected on a Hewlett-Packard 8452A diode array spectrophotometer with 2 nm step size for 10 μM peptide in 10 mM sodium phosphate buffer, 150 mM NaCl (pH 7.0) at room temperature, unless stated otherwise. Peptide concentrations were determined by UV/Vis spectroscopy using extinction coefficient values from the literature for δ- and ψ-containing peptides where there is no contribution from the thioamide at the absorption maximum (δ: ε_{385} = 5700 M^{-1} cm^{-1}, ψ: ε_{494} = 68,000 M^{-1} cm^{-1}).[5, 6] For F*- and μ-containing peptides, literature values were used for the extinction coefficients of the oxopeptides (F*: ε_{232} = 13,000 M^{-1} cm^{-1}, ε_{266} = 2049 M^{-1} cm^{-1}; μ: ε_{266} = 1830 M^{-1} cm^{-1}, ε_{324} = 12,000 M^{-1} cm^{-1}), and a combination of direct weighing of the peptides and checking UV/Vis spectra for self-consistency was used to determine the following extinction coefficients: ZPPPPA^{s}A^{s}G: ε_{266} = 14,172 M^{-1} cm^{-1}, ZPPPP^{s}A^{s}A^{s}G: ε_{266} = 18,298 M^{-1} cm^{-1}, where the extinction coefficient of the fluorophore Z would be added to these values to get the extinction coefficient for the full di- or trithiopeptide.[7, 8] The absorption spectra of FPPPPA^{s}A^{s}G (**29**) and FPPPP^{s}A^{s}A^{s}G (**30**) were used to confirm the ZPPPPA^{s}A^{s}G dithioamide and ZPPPP^{s}A^{s}A^{s}G trithioamide extinction coefficients, respectively. Spectra are shown in the main text and Figs. S12-S14.

Fluorescence Spectroscopy. Steady-state and fluorescence lifetime measurements were made using a PTI QuantaMaster 40 fluorometer with a multicell holder and Peltier temperature control at 25 °C in 1 cm quartz cuvettes. The QuantaMaster 40 was equipped with a subtractive double monochromator with an MCP-PMT (Hamamatsu Photonics R2809U; Bridgewater, NJ, USA), and a time correlated single photon counting (TCSPC) computer board (Becker and Hickl SPC-630; Berlin, Germany). Conditions for steady-state fluorescence were as follows: F*-containing peptides, λ_{ex} = 240 nm; μ-containing peptides, λ_{ex} = 333 nm; δ-containing peptides, λ_{ex} = 385 nm; ψ-containing peptides, λ_{ex} = 480 nm; all data were collected with 3 nm slit widths for excitation and emission, 1 nm step size, and 0.5 sec integration time. TCSPC measurements of fluorescence lifetimes were collected using LEDs with 340 nm (μ-peptides), 386 nm (δ-peptides), or 486 nm (ψ-peptides) excitation. Emission was collected at 393 nm (μ-peptides), 420 nm (δ-peptides), or 515 nm (ψ-peptides) at 20 °C with the following settings: 20 nm slit widths, 0-199 ns, peak channel count 10000. All spectra were collected with 5 μM peptide in 10 mM sodium phosphate buffer, 150 mM NaCl (pH 7.0), unless stated otherwise. Fits to single or double exponential functions were performed with FelixGX software as previously described.[9] Steady state

spectra are shown in the main text and Figs. S12-S14. Lifetime data from these mono- and biexponential fits are shown as insets in the steady state spectra and expanded lifetime plots showing residuals for data fitting are shown in Fig. S15. Lifetimes and fitting χ^2 values are reported in Table S2.

Since we expected that the peptides would adopt multiple conformations, we also fit the lifetime data to distributed exponential functions in order to determine whether we could observe quenched and unquenched populations. The TCSPC data for each fluorophore were fit using PTI PowerFit-10 with the Exponential Series Method. Fits for each sample were performed over the same time windows in the decay curves as for the mono- and bi-exponential fits. The fits were performed using 100 distinct lifetime values over a range which varied for each fluorophore. The resulting lifetime distributions were fit to gaussian functions (KaleidaGraph; Synergy Software; Reading, PA, USA) of the following form.

$$y = m_1 exp\left(-\left[\frac{x - m_2}{m_3}\right]^2\right) + m_4 exp\left(-\left[\frac{x - m_5}{m_6}\right]^2\right) \quad \text{(S1)}$$

All of the variables $m_{1\text{-}6}$ were allowed to freely vary during fitting. Although we did observe some shorter lifetime components, the changes in overall lifetimes were dominated by a shortening of the longer lifetime component consistent with the values obtained from the single exponential fits. Six example fits are shown in Fig. S16.

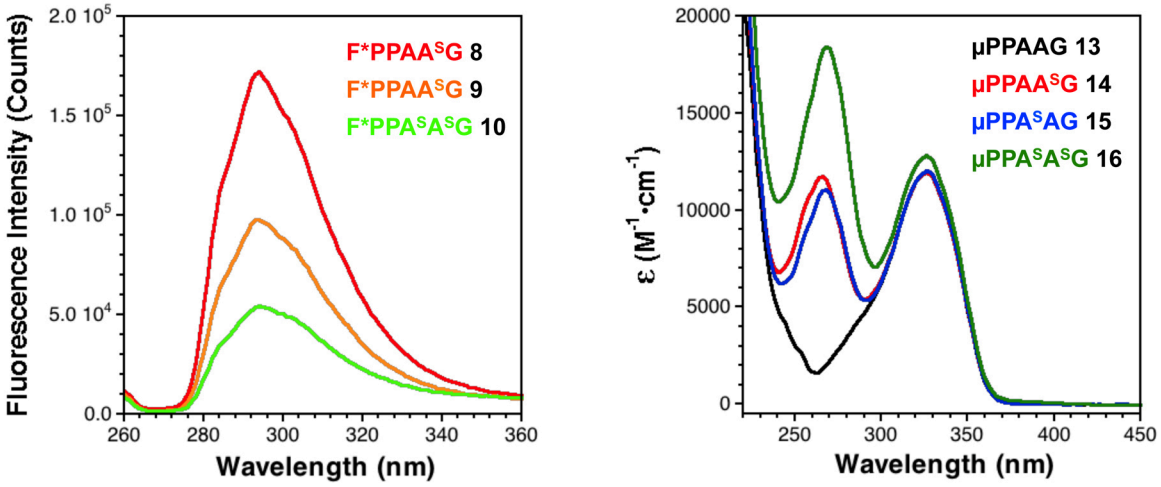

Fig. S12 Spectral Characterization of F*- and μ-Containing Peptides. Left: Fluorescence emission spectra of **8-10** at 5 μM in 10 mM sodium phosphate buffer with 150 mM NaCl (pH 7.0) at 25 °C. Excitation at 240 nm. Right: UV/Vis absorption spectra of μ-containing peptides **13-16** at 10 μM in the same buffer at 25 °C. Concentrations determined as described above.

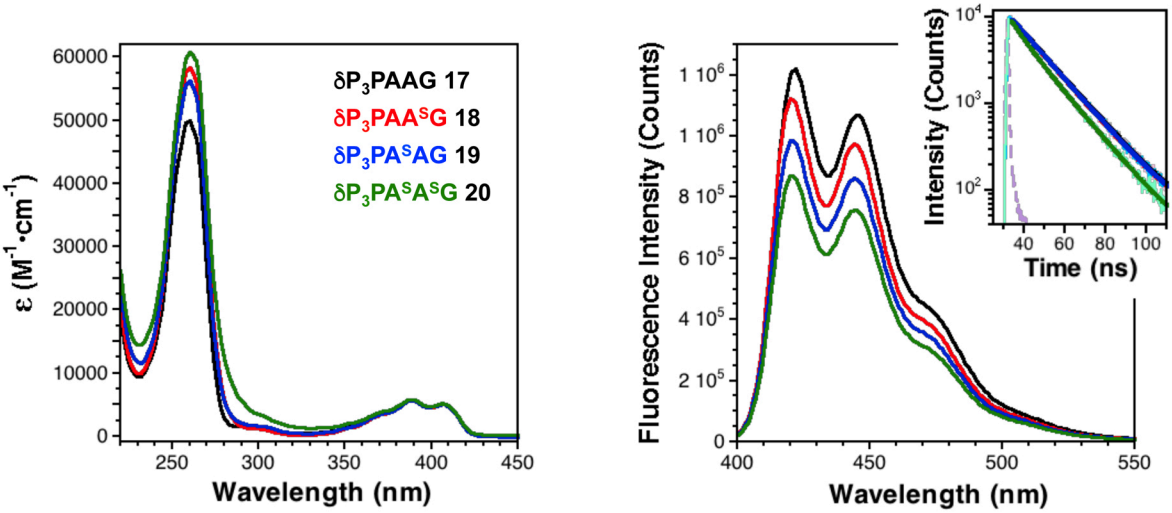

Fig. S13 Spectral Characterization of δ-Containing Peptides. Left: UV/Vis absorption spectra of δ-containing peptides **17**-**20** at 10 μM in 10 mM sodium phosphate buffer with 150 mM NaCl (pH 7.0) at 25 °C. Peptide concentrations were determined by extinction coefficient ε_{388} = 5700 M^{-1} cm^{-1} for the acridone chromophore.[6] Spectral broadening of the 270 nm thioamide absorption can be clearly seen in the 280-350 nm range. Right: Fluorescence emission spectra of **17**-**20** at 5 μM in the same buffer. Excitation at 385 nm. Inset: Fluorescence lifetimes measured using TCSPC with excitation at 386 nm. Fits to single exponential functions are shown.

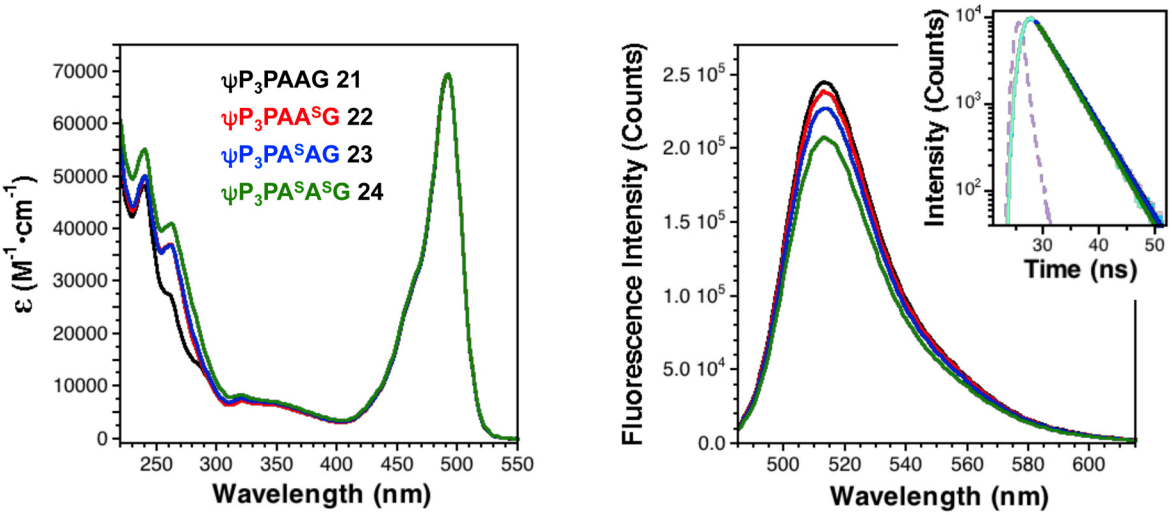

Fig. S14 Spectral Characterization of Fluorescein-Containing Peptides. Peptides labelled with fluorescein maleimide reacted with N-terminal Cys (ψ). Left: UV/Vis absorption spectra of ψ-containing peptides **21**-**24** at 5 μM in 10 mM sodium phosphate buffer with 150 mM NaCl (pH 7.0) at 25 °C. Peptide concentrations were determined by extinction coefficient ε_{494} = 68,000 M^{-1} cm^{-1} for the fluorescein chromophore.[5] Right: Fluorescence emission spectra of **21**-**24** at 1 μM in the same buffer. Excitation at 480 nm. Inset: Fluorescence lifetimes measured using TCSPC with excitation at 486 nm. Fits to single exponential functions are shown.

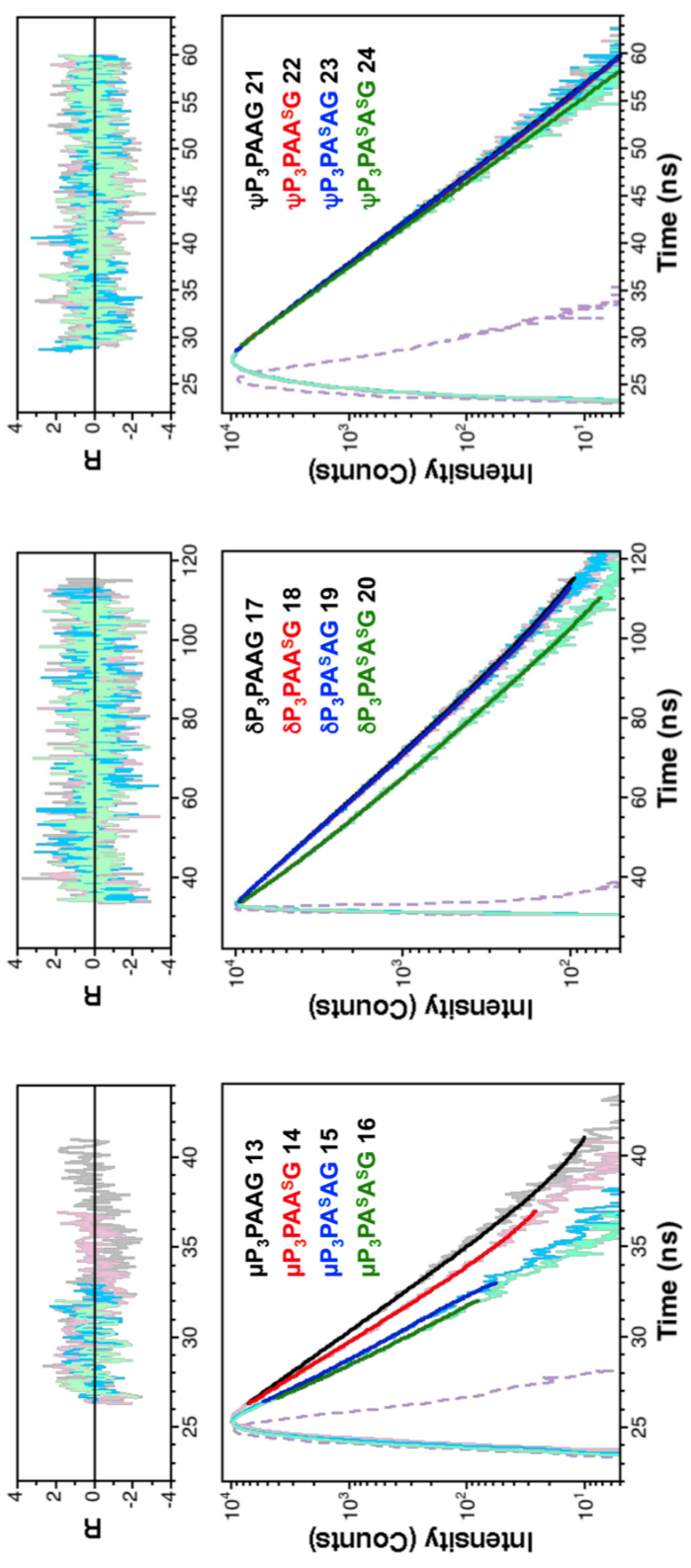

Fig. S15 Fluorescence Lifetime Measurements of Peptides **13-24**. Lifetime measurement with 5 μM peptides in 20 mM sodium phosphate buffer with 200 mM NaCl (pH 7.6) at 25 °C. Light purple line is the instrumental response function. Bold lines are single exponential fits to the data. Residuals from the fits are shown above.

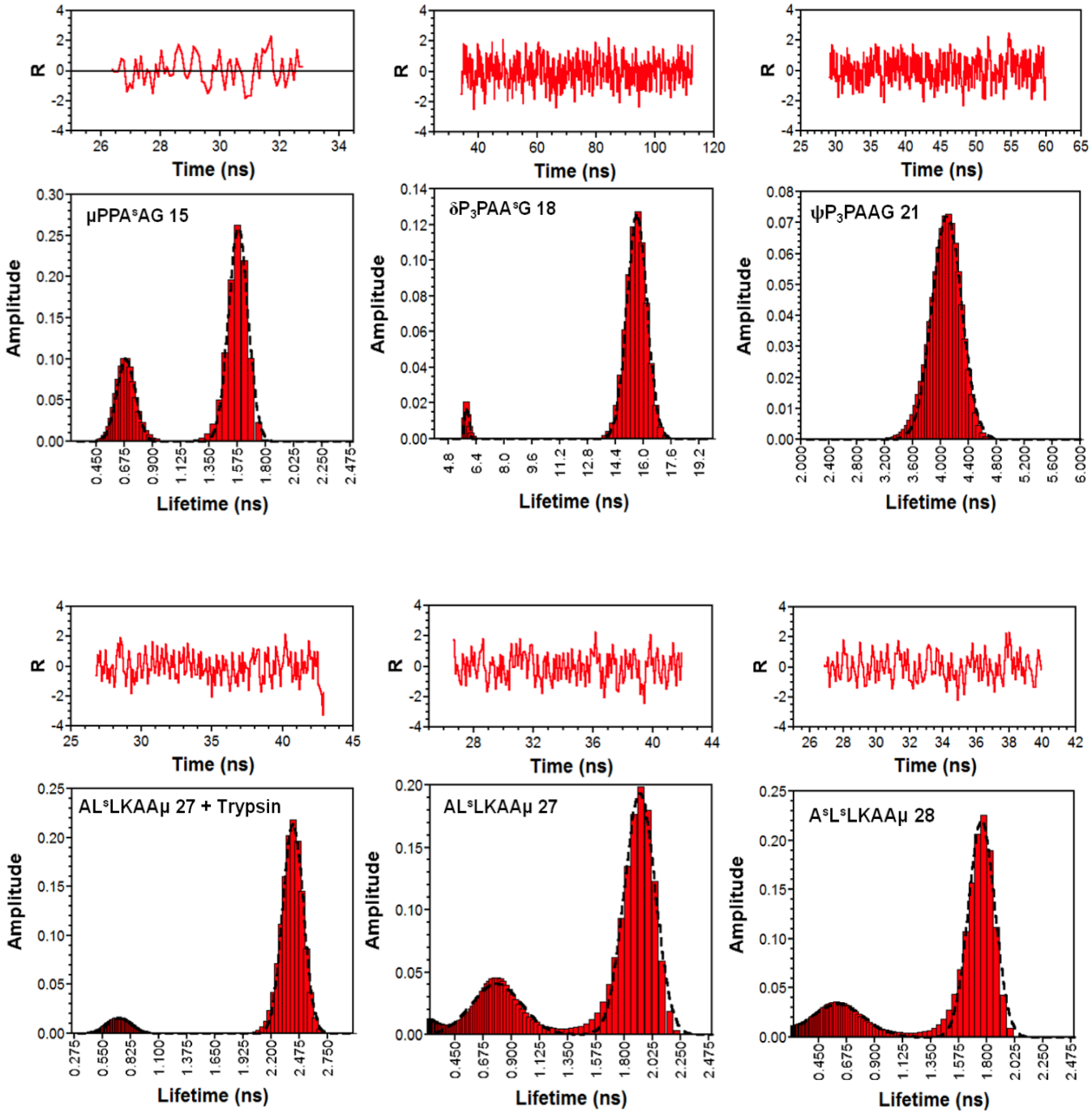

Fig. S16 Distributed Exponential Fits to Fluorescence Lifetime Data. Fitting to distributed functions performed as described using PowerFit-10, distribution profiles were then fit to one or two gaussian functions. Residuals from distributed fits are shown above the histograms. Lifetime data used in fitting can be seen in Fig. S15.

Table S2. Peptide Fluorescence Lifetimes.

Peptide	τ (ns), χ^2	Peptide	τ (ns), χ^2
μPPAAG (**13**)	2.00[a], 1.165	ψP_3PA^sAG (**23**)	3.89[a], 0.975
μPPAA^sG (**14**)	1.73[a], 1.029	ψP_3P$A^s$$A^s$G (**24**)	3.73[a], 1.057
μPPA^sAG (**15**)	1.33[b], 0.955	ALLKAAμ (**25**)	2.35[a], 0.976
μPP$A^s$$A^s$G (**16**)	1.29[a], 1.210	A^sLLKAAμ (**26**)	1.97[a], 0.990
δP_3PAAG (**17**)	15.5[a], 1.116	AL^{s}LKAAμ (**27**)	1.81[a], 0.975
δP_3PAA^{s}G (**18**)	15.2[a], 1.182	A^sL^{s}LKAAμ (**28**)	1.64[a], 1.057
δP_3PA^sAG (**19**)	15.3[a], 1.186	ALLKAAμ (**25**) + Trypsin	2.37[a], 1.079
δP_3P$A^s$$A^s$G (**20**)	11.8[a], 1.147	A^sLLKAAμ (**26**) + Trypsin	2.35[a], 1.141
ψP_3PAAG (**21**)	4.02[a], 0.976	AL^{s}LKAAμ (**27**) + Trypsin	2.37[a], 1.017
ψP_3PAA^{s}G (**22**)	3.80[a], 0.990	A^sL^{s}LKAAμ (**28**) + Trypsin	2.34[a], 1.158

[a]Lifetimes derive from fits to single exponential functions.

[b]Lifetimes derive from fits to double exponential functions. The intensity-weighted average lifetime is reported.

Table S3. Fluorescence Quenching Efficiencies in Thiopeptides[a,b,c]

Peptide	E_Q^{SS}, E_Q^{τ} (%)	Peptide	E_Q^{SS}, E_Q^{τ} (%)
μP_3P^{s}AAG (**2**)	26, ND	μPPA^sAG (**14**)	40, 34
μP_3PA^sAG (**3**)	13, ND	μPPAA^sG (**15**)	16, 14
μP_3PAA^{s}G (**4**)	7, ND	μPP$A^s$$A^s$G (**16**)	54, 36
μP_3P$A^s$$A^s$G (**5**)	29, ND	δP_3PA^sAG (**18**)	10 (8), 2
μP_3P^{s}AA^{s}G (**6**)	32, ND	δP_3PAA^{s}G (**19**)	20 (22), 1
μP_3P^s$A^s$$A^s$G (**7**)	40, ND	δP_3P$A^s$$A^s$G (**20**)	29 (32), 24
F*PPA^sAG (**9**)	40, ND	ψP_3PA^sAG[b] (**22**)	5 (4), 5
F*PP$A^s$$A^s$G (**10**)	63, ND	ψP_3PAA^{s}G[b] (**23**)	7 (8), 3
		ψP_3P$A^s$$A^s$G[b] (**24**)	15 (18), 7

[a]Steady state $E_Q^{SS} = 1 - F/F_0$, where F is the integrated fluorescence emission intensity of the thiopeptide and F_0 is the integrated intensity of the corresponding oxopeptide. Lifetime $E_Q^{\tau} = 1 - \tau / \tau_0$, where τ is the fluorescence lifetime of the thiopeptide and τ_0 is the lifetime of the corresponding oxopeptide.

[b]ψ represents fluorescein maleimide attached at N-terminal Cys residue.

[c]All experiments on peptides **2**-**7**, **9**, **10**, and **14**-**16** performed at 5 μM peptide concentration. Experiments on peptides **18**-**20** performed at 10 μM peptide concentration (additional steady state values at 1 μM). Experiments on peptides **21**-**24** performed at 5 μM peptide concentration (additional steady state values at 0.5 μM).

Spectral Overlap Calculations. The Förster distance, R_0, is given in Å by Equation (S2)

$$R_0^6 = \frac{9000(\ln 10)\kappa^2 \Phi_D J}{128\pi^5 n^4 N_A} \quad \text{(S2)}$$

where κ^2 is a geometrical factor that relates the orientation of the donor and acceptor transition moments, Φ_D is the quantum yield of the donor, n is the index of refraction of the solvent, N_A is Avogadro's number, and J is the spectral overlap integral defined in units of $M^{-1}\bullet cm^{-1}\bullet nm^4$. J is formally defined as

$$J = \int_0^\infty f_D(\lambda)\varepsilon_A(\lambda)\lambda^4 \, d\lambda \quad \text{(S3)}$$

where $\varepsilon_A(\lambda)$ is the molar extinction coefficient of the acceptor at each wavelength λ and $f_D(\lambda)$ is the normalized donor emission spectrum given by

$$f_D(\lambda) = \frac{F_{D\lambda}(\lambda)}{\int_0^\infty F_{D\lambda}(\lambda) d\lambda} \quad \text{(S4)}$$

where $F_{D\lambda}(\lambda)$ is the fluorescence of the donor at each wavelength λ. Fluorescence spectra were integrated to calculate $f_D(\lambda)$. UV/Vis spectra (with the fluorophore contribution subtracted as indicated) were used to determine $\varepsilon_A(\lambda)$. J values obtained using Equation (S3) for various donor/acceptor pairs are given in Table S4. Substituting these results into Equation (S2), as well as literature values for the donor quantum yields $\Phi_D(F^*) = 0.11$ and $\Phi_D(\mu) = 0.18$), 1.33 for the index of refraction of water, and 2/3 for κ^2 gives the Förster distances listed in Table S4.[7, 8]

Table S4. Förster Theory Calculations.[a]

Peptide	J ($M^{-1}\bullet cm^{-1}\bullet nm^4$), R_0 (Å)	Peptide	J ($M^{-1}\bullet cm^{-1}\bullet nm^4$), R_0 (Å)
F*PPA^{s}A^{s}G (**10**)	1.37 x 10^{13}, 17.5	μP$_3$PA^{s}A^{s}G (**5**)	2.88 x 10^{12}, 14.6
F*P$_3$PA^{s}A^{s}G (**11**)	1.66 x 10^{13}, 18.0	μP$_3$P^{s}A^{s}A^{s}G (**7**)	1.11 x 10^{13}, 18.3
F*P$_3$P^{s}A^{s}A^{s}G (**12**)	3.56 x 10^{13}, 20.5		

[a]Spectral overlap calculated using difference spectra of the following peptides: **8** with spectra of **10**, **11**, and **12**; **1** with spectra of **5** and **7**.

Electronic Structure Analysis.

Quantum Mechanical Calculations. Calculations were performed on thioglycine monomers capped with an N-terminal thioactyl group and a C-terminal amide to generate a minimal structure containing the dithioamide motif. The impact of n-to-π * interactions on the electronic excitation of the dithioamide moiety was assessed by comparing transitions within a structure arranged in an all *trans* conformation to transitions in a structure including a thiocarbonyl n-to-π* interaction. The all *trans* structure was generated by setting all backbone dihedral angles to 180°, while the n-to-π * structure was generated using data for bond angles, bond lengths, and dihedral angles from the crystal structure of (*S*)-1-ethanethioylpyrrolidine-2-carbothioamide in Newberry *et al*. 2013.[10] During geometry optimization, backbone dihedral angles were frozen for the all-*trans* structure, while the atomic positions of both thionyl carbon and sulfur atoms were frozen for the n-to-π * structure. The input files showing precisely which coordinates were restrained are included on the following pages. These structures were optimized at the B3LYP level of theory with a cc-pVTZ basis set in GAUSSIAN 09 (Gaussian, Inc.; Wallingford CT).[11] CIS(D) single point energies were then calculated using an aug-cc-pVTZ basis set to determine the energies and molecular orbitals involved in the lowest energy transitions for each structure. For the all-*trans* conformation, excited state 3 (f=0.2559) has an energy of 4.93889 eV and a corresponding absorption of 251 nm after CIS(D) correction. The dominant transition (determined based on oscillator strengths) of this excited state is from occupied molecular orbit (MO) 42 to unoccupied MO 58. This corresponds to a π-π * transition within one of the thioamide groups (Fig. S17). A significant contribution also comes from the transition from MO 40 to MO 55, which corresponds to a similar transition in the other carbonyl. The the third excited state (f=0.980) for the conformer containing the n-to-π* interaction has an energy of 4.6089 eV and corresponding absorption of 269 nm after CIS(D) correction, as well as distinct electron density for the dominant ground state of the transition (Fig. S18). The occupied ground state MO 43 for the transition featuring the highest oscillator strength shows significant electron density shared between the two thioamide groups. The corresponding excited state MO 57 for this transition shows that the density migrates in both thioamides. Although the calculated energies for the π-to-π* transitions are higher (as is common for CIS excitation energies), the trend is consistent with our experimental observations in that a distinct lower energy transition exists for two thioamide groups featuring an n-to-π* interaction compared to a conformer in which these two groups do not interact.

all-trans Conformation

```
---------------------------------------------------
# opt b3lyp/cc-pvtz geom=(modredundant,connectivity)
---------------------------------------------------
 C                    -2.21533   0.23785   0.00001
 C                    -3.02146   1.51356   0.00000
 H                    -2.78647   2.11265   0.88317
 H                    -2.78196   2.11583  -0.87978
 H                    -4.08132   1.28642  -0.00298
 N                    -0.8918    0.43052   0.00000
 H                    -0.49291   1.3653   -0.00011
 C                     0.07805  -0.62891   0.00000
 C                     1.50616  -0.10307  -0.00001
 H                    -0.0718   -1.27277   0.87354
 H                    -0.07182  -1.27276  -0.87354
 N                     2.41505  -1.08227  -0.00001
 C                     3.85278  -0.87397  -0.00002
 H                     2.0836   -2.03436   0.00002
 H                     4.15881  -0.31009  -0.88117
 H                     4.34108  -1.84551  -0.00013
 H                     4.15887  -0.31028   0.88124
 S                    -2.91975  -1.27131   0.00001
 S                     1.89975   1.51225  -0.00002

 The following ModRedundant input section has been read:
 D       2       1       6       8 F
 D      19       9      12      13 F
 D       6       8       9      19 F
 D      18       1       6       8 F
 D       1       6       8       9 F
 D       6       8       9      12 F
 D       8       9      12      13 F

---------------------------------------------------
# cis(d)/aug-cc-pvtz geom=(connectivity)
---------------------------------------------------

Excited State   1:      Singlet-A      4.4456 eV  278.89 nm  f=0.0002

Excited State   2:      Singlet-A      4.6334 eV  267.59 nm  f=0.0000

Excited State   3:      Singlet-A      5.9261 eV  209.22 nm  f=0.2559
      40 -> 55         0.18868
      42 -> 47         0.11771
      42 -> 49        -0.17692
      42 -> 58         0.51777
      42 -> 64         0.24155

*********************************************************************
CIS(D) Correction to the CiSingles state  3
*********************************************************************
CIS     Exc. E:  0.217778967755     a.u.     5.92607 eV   209.21833 nm
CIS(D) doubles : -0.144867068110
CIS(D) triples :  0.108589007880
CIS(D) Total   : -0.362780602296E-01        E(CIS(D))=  -1100.71404019
CIS(D) Exc. E:  0.181500907525     a.u.     4.93889 eV   251.03650 nm
```

n-to-π^* Conformation

```
---------------------------------------------------
# opt b3lyp/cc-pvtz geom=(connectivity)
---------------------------------------------------
 C                  -1    1.91944   0.06703   0.09478
 C                   0    3.16317  -0.63631  -0.36505
 H                   0    3.63824  -1.19404   0.44515
 H                   0    2.89417  -1.34375  -1.15333
 H                   0    3.86838   0.07790  -0.77733
 N                   0    1.21268  -0.57342   1.04384
 H                   0    1.47018  -1.52294   1.25977
 C                   0   -0.09615  -0.14036   1.47592
 C                  -1   -1.17441  -0.24581   0.39283
 H                   0   -0.39431  -0.77494   2.31226
 H                   0   -0.02610   0.88980   1.83075
 N                   0   -2.17392   0.62462   0.52277
 C                   0   -3.30502   0.70717  -0.38466
 H                   0   -2.04999   1.38192   1.17632
 H                   0   -3.80103  -0.25950  -0.45096
 H                   0   -2.97744   0.98659  -1.38712
 H                   0   -4.00007   1.45261  -0.00443
 S                  -1    1.38883   1.52147  -0.55233
 S                  -1   -1.07230  -1.43162  -0.79143

---------------------------------------------------
# cis(d)/aug-cc-pvtz geom=(connectivity)
---------------------------------------------------

Excited State   1:      Singlet-A      4.3833 eV  282.86 nm  f=0.0001

Excited State   2:      Singlet-A      4.4603 eV  277.97 nm  f=0.0002

Excited State   3:      Singlet-A      5.6657 eV  218.83 nm  f=0.0980
      40 -> 56         0.10700
      40 -> 58        -0.23164
      40 -> 60        -0.10425
      41 -> 54         0.10294
      41 -> 56         0.12531
      41 -> 57         0.19988
      43 -> 44        -0.10868
      43 -> 47        -0.12258
      43 -> 54         0.16206
      43 -> 56         0.13953
      43 -> 57         0.30528
      43 -> 58         0.14954
      43 -> 59         0.10701

*********************************************************************
 CIS(D) Correction to the CiSingles state  3
 *********************************************************************
 CIS     Exc. E:  0.208212209126     a.u.     5.66574 eV   218.83132 nm
 CIS(D) doubles : -0.148733552942
 CIS(D) triples :  0.109895394715
 CIS(D) Total   : -0.388381582276E-01        E(CIS(D))=  -1100.72217512
 CIS(D) Exc. E:  0.169374050898     a.u.     4.60890 eV   269.01023 nm
```

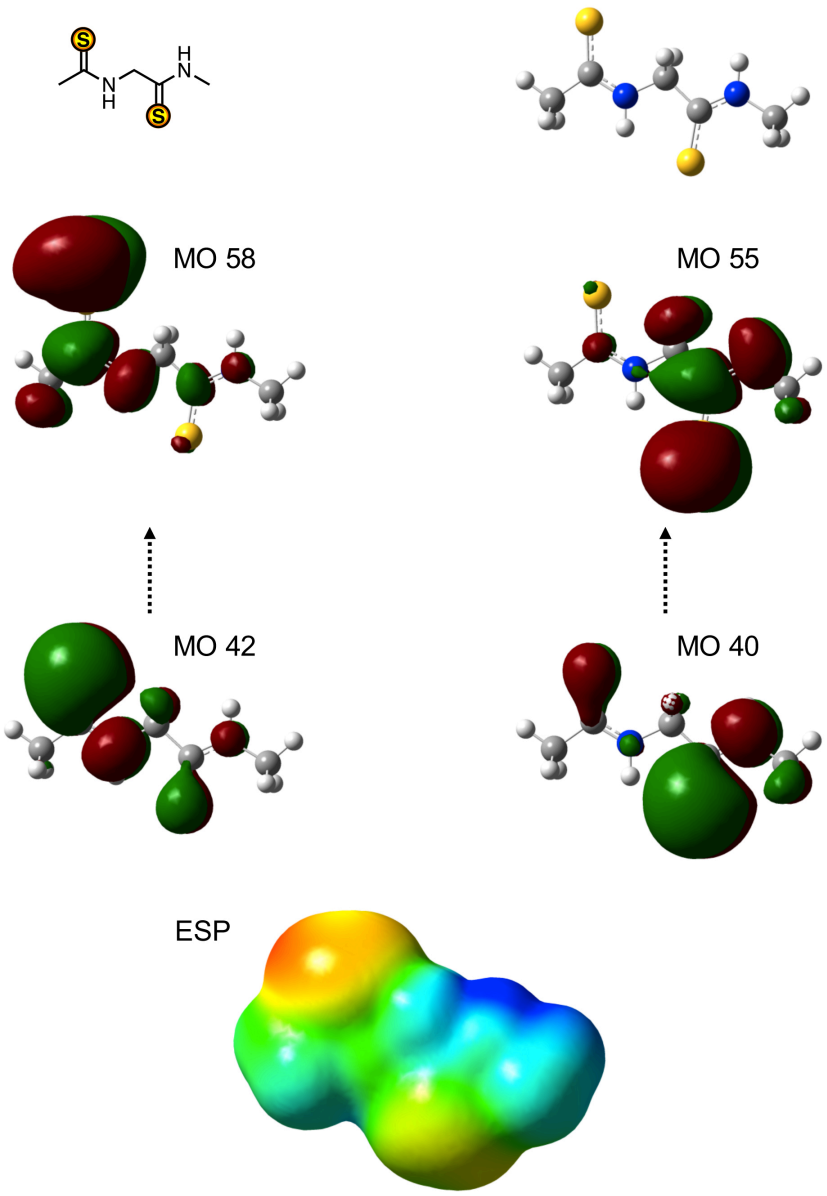

Fig. S17 Molecular Orbitals for All-*trans* Thioacetyl Thioglycyl Methyl Amide. From top: Line drawing and B3LYP optimized structure, excited state transitions between ground state MO 42 and excited state MO 58, or ground state MO 40 and excited state MO 55, and ground state electrostatic potential surface (ESP). Orbitals relevant to the spectroscopic transitions studied are shown with colors denoting positive and negative portions of the wavefunction. Orbitals generated from CIS(D)/aug-cc-pVTZ calculations and rendered using Gaussview 5.0 with orbital isovalues of 0.02 $(e^{-}/A^{3})^{1/2}$. ESP shown with the same isovalues, color scaling ranging from – 0.05 au (red) to + 0.05 au (blue).

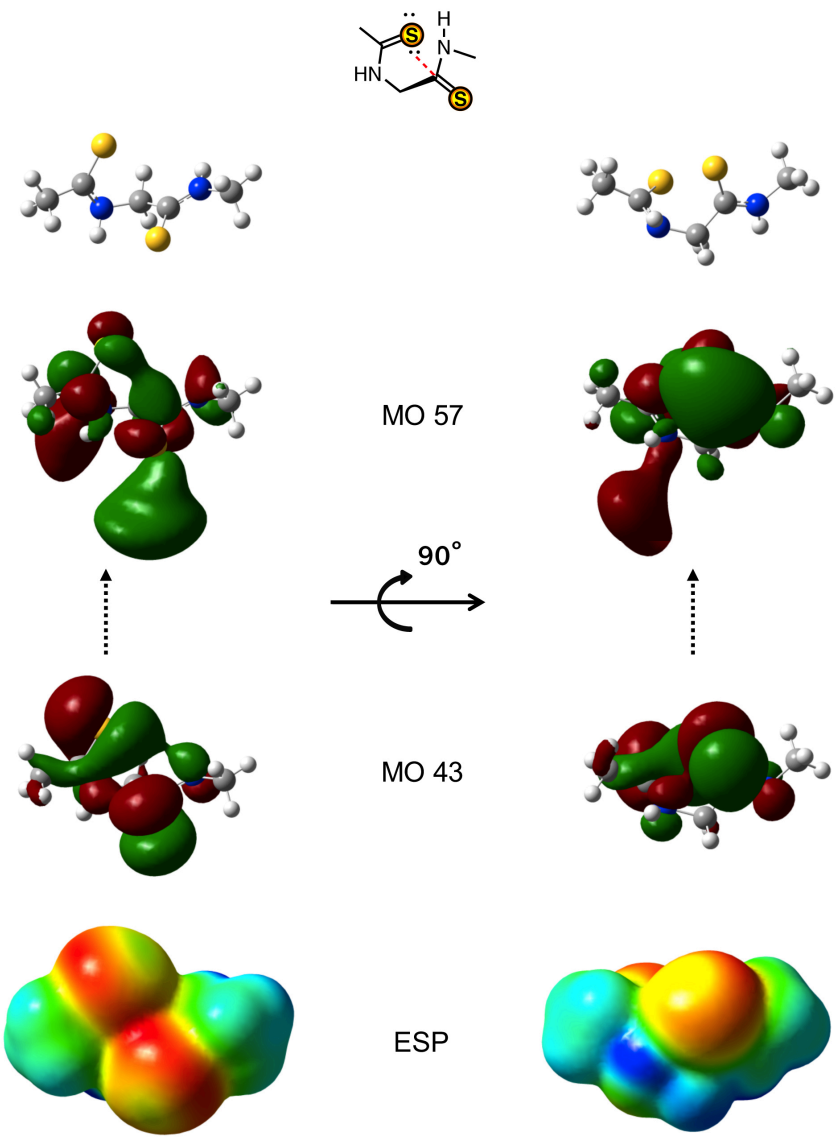

Fig. S18 Molecular Orbitals for n-to-π* Thioacetyl Thioglycyl Methyl Amide. From top: Line drawing and B3LYP optimized structure, excited state transition ground state MO 43 and excited state MO 57, and ground state electrostatic potential surface (ESP). All structure images are shown in two orientations, rotated by 90°, for clarity. Orbitals relevant to the spectroscopic transitions studied are shown with colors denoting positive and negative portions of the wavefunction. Orbitals generated from CIS(D)/aug-cc-pVTZ calculations and rendered using Gaussview 5.0 with orbital isovalues of 0.02 $(e^{-}/A^{3})^{1/2}$. ESP shown with the same isovalues, color scaling ranging from – 0.05 au (red) to + 0.05 au (blue).

Additional Discussion of Förster Resonance Energy Transfer. In calculating the Förster distances for Förster resonance energy transfer (FRET) in Table S4, we treated the polythioamides as acting as a single chromophore unit. However, as noted briefly in the main text, it is likely that n-to-π* conformers of the dithiopeptides are only a subset of the conformational ensemble. Indeed, the fact that quenching by the dithioamide moieties is not significantly different than the sum of the quenching by the corresponding monothioamides implies that n-to-π* conformers make only minor contributions. A two state conformational ensemble model, is represented below, in which FRET in one state would occur between the fluorophore and each thioamide individually, and FRET in the other state would be between the fluorophore and the n-to-π* conformer, acting as a single chromophore. Physically, the R_0 value for the n-to-π* dithioamide unit would be a distance measured from the center of the electronic transition dipole for the fluorophore to the center of the electronic transition dipole for the excited state shown in Fig. S18. The R_0 values for each of the individual thioamides would be distances measured from the center of the electronic transition dipole for the fluorophore to the centers of the electronic transition dipoles for each of the thioamides, calculated previously by our laboratory.[12]

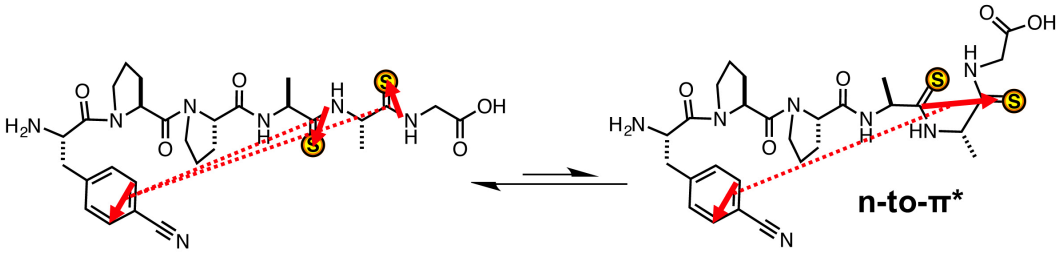

The absorption spectra used in calculating the overlap integral represent some combination of the spectra of these two populations, only one which includes n-to-π* interactions. We do not currently have a way of experimentally forcing the i, i+1 dithiopeptides into an exclusively n-to-π* conformation. In addition, since we do not know what fraction of the total conformational ensemble includes n-to-π* interactions, we cannot deconvolute the absorption spectra to attempt to determine the Förster distance for the n-to-π* population alone. The values in Table S4 therefore represent lower bounds for the n-to-π* conformer R_0 with a substantial contribution from the individual thioamides acting as single chromophores. In practice, deconvoluting these contributions may be extremely difficult, but could be possible once an appropriate model system can be used to determine the extinction coefficient for a purely n-to-π* dithioamide chromophore.

Additional Discussion of Photoinduced Electron Transfer. The electronic interaction observed in the calculated structures shown in Fig. S18 is also likely to decrease the oxidation potential of the thioamide, improving its ability to act as a quencher through photoinduced electron transfer (PET). PET can occur through a static or dynamic mechanism, or both. Static quenching results from the formation of a ground state complex between the fluorophore and the quencher, preventing excitation of the fluorophore. Dynamic quenching involves electron transfer to or from the excited state of the fluorophore, resulting in a non-radiative return to the ground state that shortens the excited state (fluorescence) lifetime of the fluorophore. Since static quenching prevents excitation of the fluorophore, it does not affect the lifetimes of those fluorophore molecules that are successfully excited. Thus, our TCSPC measurements showing shortened fluorophore lifetimes provide clear evidence of dynamic quenching for all of the thiopeptides studied. For dynamic quenching, the Gibbs free energy of PET (ΔG_{ET}) is given by Equation S5[13]

$$\Delta G_{ET} = N_A e\left(E^{\circ}_{D^+/D} - E^{\circ}_{A/A^-}\right) - E_{0,0} + C \qquad \text{(S5)}$$

where N_A is Avogadro's number; e is the elementary charge; $E^{\circ}_{D+/D}$ and $E^{\circ}_{A/A-}$ are the standard electrode potentials of the donor (thioamide) and acceptor (fluorophore) moieties, respectively; C is a solvent-dependent term accounting for the electrostatic work arising from the Coulombic interaction between the donor and acceptor during electron transfer, which is typically negligible in polar solvents; and $E_{0,0}$ is the vibrational zero electronic energy of the excited chromophore. If one compares PET quenching of a fluorophore by a monothioamide and a dithioamide in an n-to-π* conformer, a decreased oxidation potential for the n-to-π* dithioamide ($E^{\circ}_{D+/D}$) would yield a more favorable ΔG_{ET} for the n-to-π* dithioamide, and thus greater quenching through PET. Experimental measurements of the oxidation potential for the n-to-π* dithioamide will require a constrained system that exclusively populates the n-to-π* conformer.

Although the TCSPC measurements clearly show that dynamic quenching plays a role in PET quenching in the thiopeptides, the small discrepancies between the quenching efficiencies calculated from the steady state fluorescence measurements and fluorescence lifetime measurements imply that static quenching may also play a role. Static quenching can occur either through intramolecular contacts between the fluorophore and quencher that depend on conformational dynamics, or through intermolecular contacts that depend on association of two thiopeptide molecules. In order to distinguish

between these two possibilities, we carried out steady state fluorescence measurements of peptides **17**-**24** at 10-fold lower concentrations than those used in the experiments for Fig. S13 and Fig. S14. We chose these peptides because quenching operates exclusively through a PET mechanism for δ and ψ fluorescence. The level of quenching is essentially identical at the concentrations studied here (see Table S3). While the peptides may interact at high (mM) concentrations, these data show that there is no significant intramolecular static quenching in the low μM concentration range.

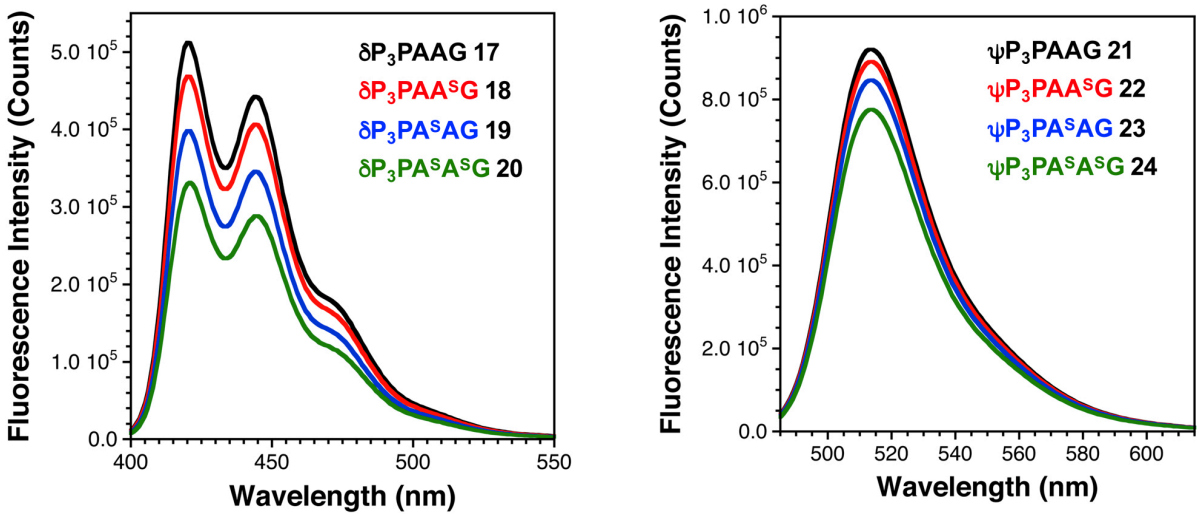

Fig. S19 Quenching in δ- and ψ-Containing Peptides at Varying Concentrations. Left: Fluorescence emission spectra of δ-containing peptides **17**-**20** at 1 μM in 10 mM sodium phosphate buffer with 150 mM NaCl (pH 7.0) at 25 °C. Right: Fluorescence emission spectra of **21**-**24** at 0.5 μM in the same buffer. Excitation at 480 nm.

Protease Assays.

Steady-State Protease Assays. Trypsin was dissolved in 1 mM HCl to make 0.5 mg/ml stock solution. The working concentration of trypsin and substrate peptides **25-28** was 5 μg/ml and 8 μM, respectively. Measurement was performed by Tecan M1000 plate reader with a 96-well plate. The excitation wavelength was 325 nm and the excitation slit width was 5 nm. The emission wavelength was 391 nm and the slit width was 5 nm. The reaction volume for each well was 50 μl. The trypsin stock solution was diluted into the working buffer (20 mM sodium phosphate, 200 mM NaCl, pH 7.6) and incubated for 5 minutes at 25 °C. The cleavage reaction was initiated by adding peptide stock solution (40 μM) into the well and the fluorescence was monitored immediately using the plate reader. Prior to addition of trypsin, and following a 1 h trypsin incubation (where proteolysis should be complete), the fluorescence lifetimes of peptides **25-28** were measured using the TCSPC system described above for μ-containing peptides (Fig. S20).

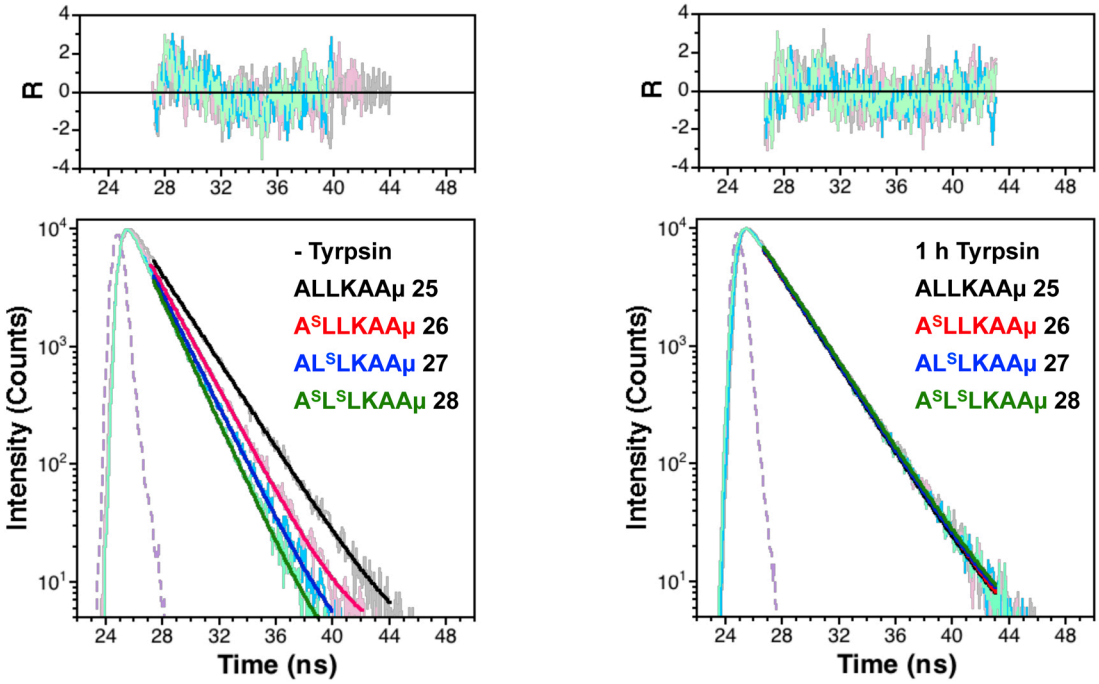

Fig. S20 Fluorescence Lifetime Measurements of Peptides **25-28**. Lifetime measurement with 5 μM peptides in 20 mM sodium phosphate buffer with 200 mM NaCl (pH 7.6) at 25 °C in the absence (left) or presence (for 1 h, right) of trypsin. Light purple line is the instrumental response function. Bold lines are single exponential fits to the data. Residuals from the fits are shown above.

Trypsin Digestion Analysis by HPLC. Briefly, trypsin digest reactions (200 µL total volume; 50 µM peptides, 20 mM sodium phosphate, 200 mM NaCl, pH 7.6 in the presence and absence of 5 µg/mL trypsin) at 25 °C were quenched at 100 min by addition of acetone (800 µL) to precipitate the protease. The reactions were cooled at -20 °C for 1 h and then centrifuged at 13,200 rpm at 4 °C for 20 min. Collect the supernatant in a new tube and keep the cap open to allow the acetone to evaporate overnight. The remaining solutions were dried in a vacuum centrifuge. Each sample was brought up in 0.6 mL H_2O and analyzed by HPLC with a Phenomenex Luna C8 analytical column (Torrance, CA, USA) using a linear solvent gradient that was isocratic for 2 min at 2% organic phase (0.1% TFA in MeCN) and then ramped from 2% to 60% organic phase over 30 min. Absorbance was monitored at 215 nm. MALDI-MS was used to confirm the identity of peaks (Fig. S21).

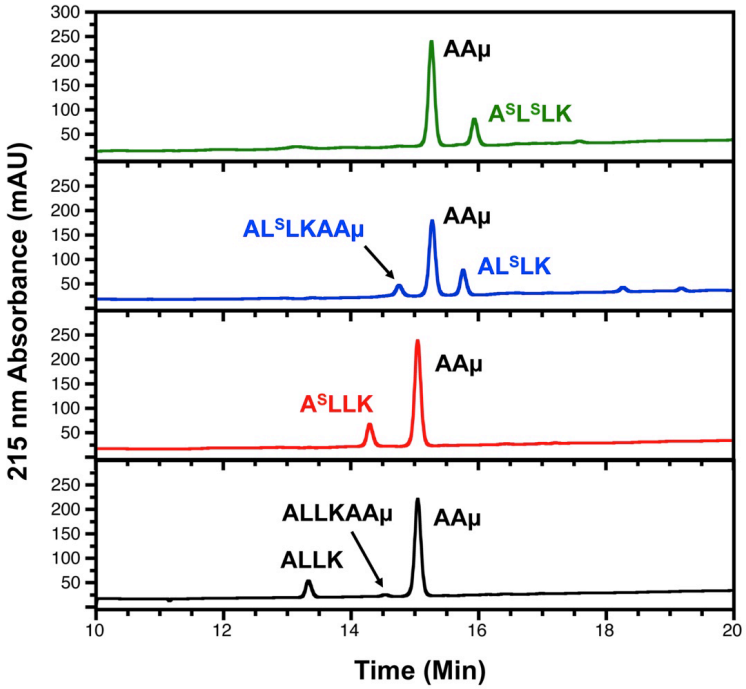

Fig. S21 HPLC Analysis of Proteolysis. HPLC Analysis of trypsin-mediated cleavage for peptide **25-28**. The traces were monitored at 215 nm. Peaks corresponding to the hydrolyzed fragments are labeled. Masses determined by MALDI-MS for each fragment match those calculated for the expected products: For AAµ calcd 406.16 $[M+H]^+$, found 406.26 $[M+H]^+$; for ALLK, calcd 444.32 $[M+H]^+$, found 466.15 $[M+Na]^+$; for A^{s}LLK calcd 460.30 $[M+H]^+$, found 460.17 $[M+H]^+$; for AL^{s}LK calcd 460.30 $[M+H]^+$, found 460.18 $[M+H]^+$; for A^{s}L^{s}LK calcd 476.32 $[M+H]^+$, found 498.20 $[M+Na]^+$.

Stopped Flow Trypsin Kinetic Measurements. Various concentrations of **28** were reacted with 25 μg/mL trypsin in sodium phosphate buffer as above at 25 °C. The fluorescence change was measured using a KinTek AutoSF-120 stopped-flow fluorometer to capture the initial phase. A plot of the average fluorescence change of three trials versus time is shown. (Fig. S22)

Since the fluorescence signal is proportional to the concentrations of **28** and the AAμ product peptide, the fluorescence of **28**, **25**, and AAμ can be expressed in Equations (S6), (S7), and (S8).

$$F_{thio} = K''_{thio}c \quad (S6)$$

$$F_{oxo} = K''_{oxo}c \quad (S7)$$

$$F_{cleaved} = K''_{AA\mu}c \quad (S8)$$

We also observed that with the same concentration of peptides, the fluorescence of **28** is 56.48% of **25**'s fluorescence, and the fluorescence of cleaved **28** (i.e., AAμ) is identical to **25**. So that

$$K''_{thio} = 0.5648 * K''_{oxo} = 0.5648 * K''_{AA\mu} \quad (S9)$$

Before **28** reacts with trypsin, the fluorescence can be expressed using Equation (S10).

$$F_0 = K''_{thio}[S] \quad (S10)$$

Here, F_0 was determined by extrapolating the y-intercept from linear regressions of the first 15 s of measured fluorescence for each reaction. K''_{thio} was determined as the slope of the linear regression of F_0 and [S].

At any given time point t of the reaction of **28** and trypsin, the fluorescence of the reaction, F, comes from the mixture of **28** and cleaved **28** (AAμ), and can be expressed with Equation (S11).

$$F = F_{AA\mu} + F_{thio} = K''_{AA\mu}[S]\chi_{AA\mu} + K''_{thio}[S](1-\chi_{AA\mu}) \quad (S11)$$

Here, $\chi_{AA\mu}$ is the mole fraction of cleaved **28** (AAμ).

Then, the fluorescence difference ΔF can be expressed with Equation (S12).

$$\Delta F = F - F_0 = (K''_{AA\mu} - K''_{thio})[S]\chi_{AA\mu} \quad (S12)$$

By combining Equations (S9) and (S12), we can further simplify Equation (S12) into (S13).

$$\Delta F = 0.7704K''_{thio}[S]\chi_{AA\mu} \quad \text{(S13)}$$

Then we can calculate the concentration of cleaved **28** using Equation (S14)

$$[AA\mu] = [S]\chi_{AA\mu} = \Delta F / 0.7704K''_{thio} \quad \text{(S14)}$$

The initial rate (v_0) was then calculated as the slope of a line fit to the first 15 s of the [AAμ] *vs*. time for each **28** cleavage reaction. The initial rates and substrate concentration were fit to the Michaelis-Menten Equation (S15) in KaleidaGraph, where $[E]_0$ is the concentration of trypsin and $[S]_0$ is the initial concentration of **28**, to obtain k_{cat} and $K_{m,app}$ (apparent) values. A plot of the Michaelis-Menten fit is shown in Figure S22.

$$v_0 = \frac{k_{cat}[E]_0[S]_0}{[S]_0 + K_{m,app}} \quad \text{(S15)}$$

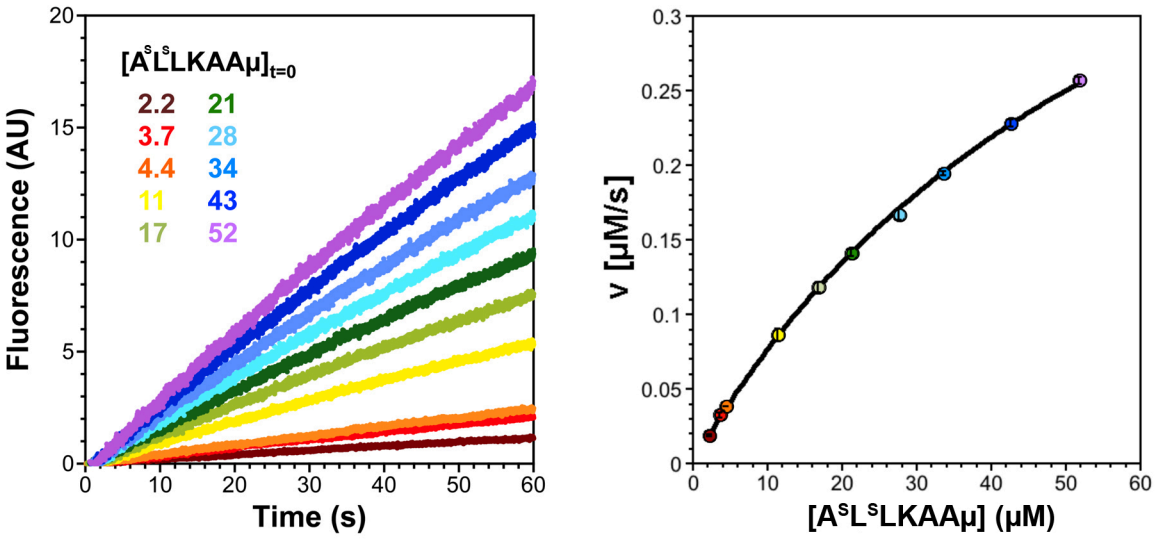

Fig. S22 Trypsin Kinetics Measurements. Left: Primary fluorescence data (average of three trials) for cleavage reactions with 25 μg/mL trypsin and varying initial concentrations of A^{S}L^{S}LKAAμ (**28**). Right: Initial rates derived from the fluorescence data plotted as a function of initial substrate concentration. The data were fit to a Michaelis-Menten model to obtain k_{cat} and $K_{m,app}$ values.

References.

1. L. C. Speight, A. K. Muthusamy, J. M. Goldberg, J. B. Warner, R. F. Wissner, T. S. Willi, B. F. Woodman, R. A. Mehl and E. J. Petersson, *J. Am. Chem. Soc.*, 2013, **135**, 18806.
2. S. Batjargal, Y. Huang, Y. J. Wang and E. J. Petersson, *J. Peptide Sci.*, 2014, **20**, 87.
3. M. A. Shalaby, C. W. Grote and H. Rapoport, *J. Org. Chem.*, 1996, **61**, 9045.
4. G. Fields, Z. Tian and G. Barany, in *Synthetic Peptides-A User's Guide*, ed. G. Grant, W. H. Freeman, New York, NY, USA, 1992, pp. 77.
5. D. Huang, A. D. Robison, Y. Liu and P. S. Cremer, *Biosens. Bioelectron.*, 2012, **38**, 74.
6. A. Szymanska, K. Wegner and L. Lankiewicz, *Helv. Chim. Acta*, 2003, **86**, 3326.
7. M. P. Brun, L. Bischoff and C. Garbay, *Angew. Chem. Int. Ed.*, 2004, **43**, 3432.
8. M. J. Tucker, R. Oyola and F. Gai, *Biopolymers*, 2006, **83**, 571.
9. J. M. Goldberg, S. Batjargal, B. S. Chen and E. J. Petersson, *J. Am. Chem. Soc.*, 2013, **135**, 18651.
10. R. W. Newberry, B. VanVeller, I. A. Guzei and R. T. Raines, *J. Am. Chem. Soc.*, 2013, **135**, 7843.
11. Gaussian 09, Revision E.01, M. J. Frisch, G. W. Trucks, H. B. Schlegel, G. E. Scuseria, M. A. Robb, J. R. Cheeseman, G. Scalmani, V. Barone, B. Mennucci, G. A. Petersson, H. Nakatsuji, M. Caricato, X. Li, H. P. Hratchian, A. F. Izmaylov, J. Bloino, G. Zheng, J. L. Sonnenberg, M. Hada, M. Ehara, K. Toyota, R. Fukuda, J. Hasegawa, M. Ishida, T. Nakajima, Y. Honda, O. Kitao, H. Nakai, T. Vreven, J. A. Montgomery, Jr., J. E. Peralta, F. Ogliaro, M. Bearpark, J. J. Heyd, E. Brothers, K. N. Kudin, V. N. Staroverov, R. Kobayashi, J. Normand, K. Raghavachari, A. Rendell, J. C. Burant, S. S. Iyengar, J. Tomasi, M. Cossi, N. Rega, J. M. Millam, M. Klene, J. E. Knox, J. B. Cross, V. Bakken, C. Adamo, J. Jaramillo, R. Gomperts, R. E. Stratmann, O. Yazyev, A. J. Austin, R. Cammi, C. Pomelli, J. W. Ochterski, R. L. Martin, K. Morokuma, V. G. Zakrzewski, G. A. Voth, P. Salvador, J. J. Dannenberg, S. Dapprich, A. D. Daniels, Ö. Farkas, J. B. Foresman, J. V. Ortiz, J. Cioslowski, and D. J. Fox, Gaussian, Inc., Wallingford CT, 2009.
12. J. M. Goldberg, S. Batjargal and E. J. Petersson, *J. Am. Chem. Soc.*, 2010, **132**, 14718.
13. D. Rehm and A. Weller, *Israel J. Chem.*, 1970, **8**, 259.